TÉCNICO LISBOA

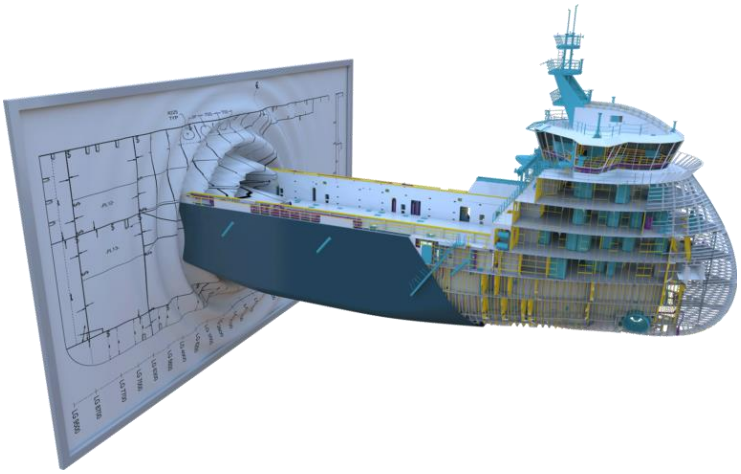

Geometric characterization of ship structural design

Ricardo Domingues Ruivo Rosa Machado

Thesis to obtain the Master of Science Degree in

Naval Architecture and Ocean Engineering

Supervisors: Prof. José Manuel Antunes Mendes Gordo

Prof. Manuel Filipe Simões Franco Ventura

Examination Committee

Chairperson: Prof. Ângelo Manuel Palos Teixeira

Supervisor: Prof. Manuel Filipe Simões Franco Ventura

Member of the Committee: Prof. Yordan Ivanov Garbatov

December 2021

TÉCNICO LISBOA

Geometric characterization of ship structural design

Ricardo Domingues Ruivo Rosa Machado

Declaração

Declaro que o presente documento é um trabalho original da minha autoria e que cumpre todos os requisitos do Código de Conduta e de Boas Práticas da Universidade de Lisboa.

Lisboa, 20 de Dezembro de 2021

Assinatura:

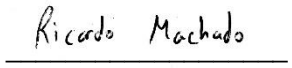

Declaration

I declare that this document is an original work of my own authorship, and it fulfils all the requirements of the Code of the University of Lisbon.

Lisbon, December 20th 2021

Signature:

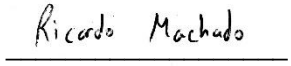

“The measure of who we are is what we do with what we have.”

- Vince Lombardi

Acknowledgements

First of all, I want to dedicate the present work to my grandmother, Adília Rosa. The constant thought of you stuck with me during the last few months and gave me the strength to finish this thesis and my degree. Just know that you'll soon have one more graduated grandson, and he'll be waiting for you to come back home as healthy as ever.

Secondly, I want to thank my family. To my mother Elsa and my father José, for always being there through thick and thin, with unconditional love and support. For shaping me into the young man I am today, pushing me to always be the best version of myself. To my brother Rafael, for all the times he knew exactly when I couldn't be disturbed and exactly when I wanted to be disturbed. Thank you for always making it so easy to unwind from my problems.

I want to particularly thank Gabriel Vieira, Tiago Amaral and Valter Moita, for helping me get through these 5 years of Técnico alive. For all the barbecues, dinners, and nights out, but also for all the lab classes, study sessions and projects carried out together. I hope one day I'll be able to make it all up to you guys.

To my friends back home, Ângelo Peixoto, Carolina Bernardino, Daniel Gomes and João Figueiredo, I want to thank you for helping me unplug from all the madness in Lisbon, and always being there for me. When you have great friends, distance really doesn't mean anything.

To all my colleagues and teachers in Delft during my ERASMUS period, I want to say thank you for not only welcoming me in the best way possible, but to give me one of the best experiences in my life. A special hug to my great friend Francesco De Simone, to whom I'm forever indebted.

Finally, I want to thank Professor José Gordo for the help and guidance throughout all my years in Técnico. His technical knowledge, helpfulness and charisma will sit with me for a very long time.

Resumo

A presente dissertação teve dois principais objetivos em vista. O primeiro foi a recolha de dados relativos à caraterização geométrica de vários navios, a nível global e local. O segundo objetivo foi o estudo acerca de como estas caraterísticas geométricas afetam variáveis importantes no projeto estrutural de navios, nomeadamente a resistência à compressão de painéis reforçados, a tensão à flexão da estrutura secundária e os custos totais de produção de painéis.

Para esta tese, duas bases de dados foram implementadas. A primeira consistiu na base de dados de navios, onde foram alocadas as características geométricas a nível global de vários navios. A segunda consistiu na base de dados de painéis de cada navio. Esta foi composta pela informação geométrica a nível local, definindo a geometria dos elementos de chapa e reforço que constituíam cada tipo de painel para cada navio considerado.

Três estudos principais foram efetuados utilizando as bases de dados recolhidas. O estudo da resistência à compressão de painéis reforçados e a avaliação da resistência à flexão da estrutura secundária permitiram compreender como a integridade estrutural do navio é afetada por variáveis a nível global e local. O estudo dos custos totais de produção de painéis levou a observações importantes acerca de como o tipo de navio ou as dimensões do mesmo afetam (ou não) a rentabilidade da produção.

Os resultados obtidos foram analisados de forma a alcançar conclusões acerca das áreas estudadas, para avaliar a importância das bases de dados e quão úteis poderão ser em estudos futuros.

.

Palavras-chave: Base de dados, Caraterização geométrica, Resistência à compressão, Resistência à flexão, Custos de produção

Abstract

This dissertation had two main goals to reach. The first was to gather a set of data consisting of the geometric characterization of several ships, at both a global and local level. The second objective was to study how these geometrical characteristics affected some of the most important structural design aspects, namely the stiffened panel strength, the local strength assessment of the secondary structure and the total panel production costs.

For this thesis, two databases were implemented. The first one consisted of the ships database, hence presenting all the global geometrical characteristics of several ships. The second one consisted of the ship panels database. As the name suggests, this comprised all the geometrical information at a local level, defining the geometry of both the plate and stiffener elements that constituted every panel type of each of the considered ships.

Three main studies were carried out using the gathered databases, focusing on structural integrity and production costs. The stiffened panel strength study and the local strength assessment allowed to evaluate how the structural integrity of the ship was affected by variables at both global and local levels. The total panel production costs assessment led to important remarks concerning how ship types and their respective dimensions affect (or not) the profitability of a newbuilding.

The obtained results were analysed to gather conclusions regarding not only the distinct disciplines under study, but to evaluate the importance of the databases and how useful they can be for further works.

Keywords: Database, Geometric characterization, Panel strength, Local strength, Production costs

Table of Contents

List of figures

List of tables

List of symbols

l	Length between frames
t_p	Plate thickness
b	Plate breadth
d_w	Web height
t_w	Web thickness
b_f	Flange breadth
t_f	Flange thickness
Y_{cg_p}	Vertical centre of gravity of the plate
Y_{cg_s}	Vertical centre of gravity of the stiffener
Y_{cg_c}	Vertical centre of gravity of the column element
d_p	Distance between the vertical centres of gravity of the plate and the column
d_s	Distance between the vertical centres of gravity of the stiffener and the column
I_{xx_p}	Second moment of area about the x-axis of the plate
I_{xx_s}	Second moment of area about the x-axis of the stiffener
I_{xx}	Second moment of area about the x-axis of the column element
E	Young's modulus
σ_0	Yield Stress
ε_0	Yield Strain
$\bar{\varepsilon}$	Average strain ratio
β	Plate slenderness
λ	Column slenderness
r	Radius of gyration
A_s	Stiffener cross section area
Φ_e	Edge stress ratio
Φ_w	Plate effective width
Φ_a	Normalised average stress of plate
Φ_E	Euler stress ratio
Φ_{jo}	Johnson-Ostenfeld contribution for the average stress of a column
Φ_{ab}	Compressive strength of a stiffened plate column
t_c	Corrosion addition thickness
t_{res}	Reserve thickness
R_x	Reaction force at point x along longitudinal axis
M_x	Moment at point x along longitudinal axis
$V(x)$	Shear force at point x along longitudinal axis
p	Lateral pressure
s	Longitudinal stiffener spacing

Z	Section modulus
l_{bdg}	Effective bending span
f_{bdg}	Bending moment factor
χ	Intact or flooded conditions coefficient
C_s	Permissible bending stress coefficient
R_{eH}	Minimum yield stress
w_p	Panel width
ρ_{steel}	Steel density
W_p	Plate weight
W_s	Stiffener weight
C_m	Material costs
l_c	Cutting length
C_c	Cutting costs
C_a	Assembly costs
$A_{w_{pp}}$	Plate-plate weld cross section area
$L_{w_{pp}}$	Plate-plate weld length
$A_{w_{ps}}$	Plate-stiffener weld cross section area
$L_{w_{ps}}$	Plate-stiffener weld length
W_w	Weld weight
C_w	Welding costs
R^2	Coefficient of determination
α	Panel aspect ratio

Glossary

ABS	American Bureau of Shipping
AIS	Automatic Identification System
BDA	Big Data Analytics
BK	Bulk Carrier vessel
BV	Bureau Veritas
CC	Container Carrier vessel
DB	Double Bottom panel
DNV	Det Norske Veritas
EEOI	Energy Efficiency Operational Indicator
FEA	Finite Element Analysis
FSA	Formal Safety Assessment
FOC	Fuel Oil Consumption
IACS	International Association of Classification Societies
IMO	International Maritime Organization
ISM	International Safety Management
LB	Longitudinal Bulkhead panel
LPP	Length between Perpendiculars
LR	Lloyd's Register
LRFD	Load and Resistance Factor Design
LS	Limit States
MARPOL	International Convention for the Prevention of Pollution from Ships
MP	Multipurpose vessel
P	Passenger vessel
PBS	Performance-Based Standards
SS	Side Shell panel
T	Tanker vessel
TPPCA	Total Panel Production Costs per unit Area
TPPCW	Total Panel Production Costs per unit Weight
TPS	Toyota Production System
UR	Unified Requirement

1. Introduction

1.1. Motivation

In recent years, most sectors of society have seen their activities impacted or completely changed with the usage of data analytics – the practice of using data to manage information and performance. This trend is no longer limited to top-end companies, as 59% of enterprises are using Big Data Analytics (BDA) to make better decisions, enable key strategic initiatives and to improve relationships with both customers and business partners [1]. A study carried out in 2018 showed that 71% of enterprises globally predict an acceleration on their investment in data and analytics over the course of the following 3-year period [2].

The maritime sector itself has experienced a shift in paradigm that led to the implementation of BDA in multiple areas. Whether due to the legislation regarding emissions, the need to become more efficient in an increasingly competitive shipbuilding market, the need to optimize existent and new routes for more viable shipping or simply to ensure more safe sailing, the maritime industry has really pushed to stay up to par with other sectors.

The regulations imposed by Annex VI of the International Convention for the Prevention of Pollution from Ships (MARPOL) concerning ship energy efficiency have led to multiple studies in order to properly estimate the Fuel Oil Consumption (FOC) for the calculation of the Energy Efficiency Operational Indicator (EEOI). Automatic Identification System (AIS) data, ship static data and environmental data are used to estimate the EEOI without requiring the actual FOC, allowing stakeholders such as the shipbuilding company and classification societies to check how efficient their ships are in actual operation [3].

Further arguments for the introduction of BDA and other technological developments in the shipping and shipbuilding industry can be made when comparing its low-tech character with either the aviation or the automotive industries, which can be seen as an employment problem for the maritime sector. Henceforth, and in order to attract the next generation of maritime professionals, the sector must focus on becoming more technologically advanced and innovative at shipyard level, while seafarers must learn new skills and integrate new technology into their know-how.

Keeping in mind the frequent instability of shipbuilding markets, shipyards should explore and underline different types of ship market, rather than specific types of the ship. This way, shipyards will be able to switch to profitable types of ship building, accordingly with the market's demands, to survive in the global market [4].

1.2. Objectives

The present thesis aims to create a database consisting of both the general characteristics of ships and the geometrical characteristic of the corresponding midship sections. The mentioned database can then be used to assess the influence of several global (ship geometry) or local (panel geometry) level parameters on several aspects, ranging from the ship's structural integrity to its building costs.

One of the main objectives of this thesis is to evaluate how the geometrical characteristics of ship structures influence the ship panel strength, in order to establish further relations regarding how the panel strength is influenced by the considered panel type, ship type or ship length. Correspondingly, a local strength assessment of secondary structure will also be implemented with respect to the gathered data. Additionally, a similar evaluation will be carried out regarding the overall production costs of ship panels, and the way how these are affected by the considered panel type or ship type.

In order to carry out this procedure, a database was designed and populated with the main structural information from several ships, gathered from midship section drawings. This database will provide a wide enough scope of panel types, ranging from bottom to deck panels, and ship types going from tankers to passenger ships. This way, a proper evaluation of the overall tendencies concerning both the ship panel strength and ship panel production costs will be ensured.

1.3. Outline

This dissertation covers the practical aspects regarding the creation of a database consisting of ship geometry and structural information. Considering the gathered information, several studies can then be carried out, in order to assess general trends and establish elation between certain variables.

In Chapter 2, the studies carried out using the data present in the gathered databases will be introduced. First, a review of the existing methods concerning the evaluation of stiffened panel strength will be presented, followed by an introduction to the method used for the local strength assessment of secondary structure. Finally, an overview of the shipbuilding industry will be executed, with an emphasis on production cost evaluation, as this will also be one of the study topics for this thesis.

The practical aspects concerning the implementation of both the ship and ship panel databases are addressed in Chapter 3. Besides, in this chapter, the formulations for the implementation of panel strength evaluation, local strength assessment and production costs evaluation are presented.

The results for panel strength, local strength assessment and production costs will be presented in Chapter 4, with variations regarding each of the main studies, to assess the influence of different variables on the findings.

Chapter 5 will comprise the main conclusions attained from the previously obtained and analyzed results. Besides, some suggestions and comments will be made concerning further work developed around the gathered databases or in this area.

2. State of the art

In the present chapter, the description of the three main aspects behind the database analysis - the approximate ultimate strength of stiffened panels, the local strength assessment of secondary structure and the parametric shipbuilding cost estimation - will be introduced to explain how important conclusions can be drawn from simple structural parameters.

Firstly, the role of classification societies on the ship structural design process is analysed. This will be done starting with an historic summary to provide a context on the standardization of rules systems, and then introducing the biggest developments over the years, and how they have been implemented or not.

Afterwards, a brief review of previously established methods that led to the most up to date formulations for the estimation of stiffened panels strength is made. After that, the presentation of each of the terms that contribute to the average stress of a column is carried out, describing the assumptions made and how these can influence the obtained results.

Then, the evaluation of the local strength of the secondary structure is introduced, with an explanation of how this assessment differs from the stiffened panel strength dealt with previously. Besides, the impact of ship length on the importance of this aspect in comparison with stiffened panels strength will be addressed.

Lastly, the several cost components that are present in the typical shipbuilding process are introduced, as well as the approach considered for the cost results analysis. Using this approach, the cost components are dealt with in a way that allows for a reasonable comparison between panels from ships with significantly different lengths and geometrical arrangements.

2.1. The role of classification societies on ship structural design

2.1.1. The International Association of Classification Societies

Most commercial ships are constructed under the rules of a classification society, such as the American Bureau of Shipping (ABS), Bureau Veritas (BV), Det Norske Veritas (DNV), Lloyd's Register (LR), among others. These and other classification societies began their activities in the 19th Century, in order to meet the growing needs of both governments and companies, while ensuring adequately reliable and safe ships.

Despite the growing independence with respect to national governments, most classification societies maintain strong links with maritime administrations in their home territories. Due to this fact, classification society rules were developed with some level of isolation for years, leading to ABS, DNV and LR

requirements (as an example) to be presented in very different ways, eventually leading to significantly different outcomes in terms of scantlings.

With the development of new technology (new ship types, higher sailing speeds, replacement of rivets by welding), regulations overseeing their use were introduced into the various standards. Other developments in analytical procedures were also incorporated as they were progressively developed. For years, the scantlings determined by LR were only proportional to displacement, which led to decreasing safety factors for larger vessels. Consequently, the rules were changed to include a more efficient consideration of wave bending. Correspondingly, local strength and stability rule requirements were at first based on successful past practices and “rules of thumb” (and later on modified, as the expertise evolved).

The differences in rules systems, and organizational issues that influenced their application, led to differences in their outcomes (in terms of both safety and reliability). The previously mentioned differences led to the establishment of the International Association of Classification Societies (IACS) in 1968, a group of the leading classification societies.

2.1.2. Developments on structural standards

IACS has worked on the development of more than 200 Unified Requirements (URs) and many Unified Interpretations and Recommendations of rule requirements. The first UR with respect to structural strength brought together the approaches of multiple classification societies on maximum wave bending moment.

Other relevant developments within the last decade have included the move towards the use of finite element analysis (FEA) to optimize scantlings, and the development of automated systems to generate and check most structural components. Some of the most relevant software systems of this type include Nauticus by DNV (used, for instance, to assess fatigue damage capacity of ship structures [5]) and Safehull by ABS (used, for instance, to investigate the time-variance of hull girder strength due to the aging of ships [6]), among many others. These software packages serve as ‘black boxes’, simplifying the work of the average ship structural designer by not requiring significant insight into the structural issues involved. The use of FEA also carries risk for the careless and for the occasional user. Besides, classification society guidance notes can only do so much as a replacement for training and experience.

The concern regarding the safety of ships all over the world was (and continues to be) one of the biggest issues with seagoing operations. Correspondingly, the International Maritime Organization (IMO) has dealt with safety problems across the entire scope of the maritime sector. The lessons were first learnt from accidents, with regulations and rules being produced subsequently to prevent similar disasters. One of the prime examples of this was the capsize of the Herald of Free Enterprise in 1987 [7]. This

tragedy greatly affected the rule-developing activities of the IMO, resulting in the adoption of the International Safety Management (ISM) code.

Formal Safety Assessment (FSA) is a recent development in structural standards. The IMO has led the improvement of this concept, describing it as "a structured and systematic methodology, aimed at enhancing maritime safety, including protection of life, health, the marine environment and property, by using risk analysis and cost-benefit assessment" [8]. The FSA procedure encompasses 5 main stages [9]:

1. Identification of dangerous sources (identify all possible dangers and find the cause and consequences of possible accidents)
2. Risk assessment and management (find the distribution of risk and the overall level of risk)
3. Risk restraining project (effective measures are implemented to reduce risk)
4. Cost and benefit evaluation (calculate the costs of each risk control)
5. Suggestions and decision (select the optimal risk control measure)

FSA was originally developed in the UK, as a response to the Piper Alpha offshore platform disaster of 1988, where 167 people lost their lives [10]. The IMO, and others, are evaluating FSA as a technique to comparatively assess the components in proposed new regulations or to compare standards. FSA allows for a cost-risk-benefit comparison to be made between the various possible issues (namely technical or human factors). FSA is being applied to the IMO rule-making process with much promise, however, the complexity of risk assessment technology translates the major obstacle in the way of a wider usage of the FSA approach.

Recently, there has been a strong movement towards what is generally described as Performance-Based Standards (PBS). These standards describe a context and safety targets that they expect the design to meet, and then leave it to the proponent to achieve the targets in any way they wish. The CSA S471 standard for offshore structures is one example of this approach [11]. In PBS, there are no specific loads or strength levels recommended. The designers are expected to demonstrate the achievement of a target level of safety by an analysis of the loads and strength. In this case, the proponent is expected to not only generate a design standard for the structure under consideration, but to also evaluate it against a risk criterion.

This approach is very popular in areas such as the offshore oil and gas industries, as it enables the approval of a wider variety of structural and system concepts (gravity-based platforms, semi-submersibles, tension-leg platforms, among others) more frequently. The obvious downside with this methodology is the divergence of designs and the potential for disagreement in safety attainment (when each of the groups involved in the project develops an essential custom design standard). Realistically, for most aspects of a design, the proponents won't have not only the resources but the time to develop a complete standard from scratch. Instead, it becomes much more practical to simply apply existing standards to ensure requirements have been met.

LRFD (Load and Resistance Factor Design) is another recent development, even though it has been used in certain standards for a few decades. It consists of a reliability-based design philosophy, which explicitly accounts for the uncertainties that occur in the determination of loads and strengths. This method was developed in the 1930's in the USSR and Europe for civil engineering purposes. Since then, LRFD has been frequently used for the design of buildings, bridges and offshore structures [12].

The goal of this procedure is to assess a consistent risk level for all comparable structures by using adjusted partial safety factors. For this, several parameters impacting the design are individually factored, to indicate both the level of uncertainty and the consequences of failure (ranging from loss of serviceability to catastrophic collapse). The approach implicitly assumes that failure is a consequence of an uncertain load exceeding an uncertain strength [13], which is a very simplistic model of an accident. LRFD has not been implemented in ship structural design due to its questionable suitability. LRFD is often implemented together with concepts from Limit States (LS) design. LS design goes beyond the intact behaviour to establish limits, both from a safety and operational perspective, so that the design reflects the boundary of undesirable behaviours. When combined, LRFD and LS design intend to correctly reflect the actual potential limits of the structure. Together, this combination intends to clarify the realistic structural risks. There are ship structural rules that have employed LS design, without LRFD. The new IACS Unified Requirements for Polar Ships [14] is one of the most relevant examples of this implementation.

2.2. Methods for the estimation of stiffened panels strength

The behaviour of stiffened plates under predominantly compressive loads is significantly difficult to describe due to the number of possible combinations of plate and stiffener geometry, boundary conditions and loads applied. The collapse load of a stiffened plate in any configuration can be precisely estimated using one of the several finite elements methodologies available. Nevertheless, and to minimize the computer power and time consumption associated with finite element modelling, simplified formulations have been frequently used for both strength assessment and design purposes. This type of approach represents the whole stiffened panel based on one isolated stiffener with an associated width of plating.

Failure of panels can be classified in four distinct modes: plate induced failure, column-like failure, tripping of stiffeners and overall grillage failure. Plate induced failure is characterized by sufficiently stocky stiffeners and a plate with a critical elastic stress lower than the yield stress. This failure mode is not frequent in ship structures, as it is mostly associated with short panels, where the width between stiffeners is approximately equal to the panel length. Column-like failure occurs due to excessive slenderness of the column, and can happen towards the plate or the stiffener, depending on the column’s initial shape and type of loading considered. Tripping of stiffeners is a consequence of a lack of torsional rigidity of the stiffeners and is one of the most dangerous failure modes due to its usual quick

shed of load carrying capacity of the column. Finally, overall grillage failure occurs in orthogonally stiffened panels (with longitudinal and transverse stiffeners) due to local buckling of the plate or of the stiffener. This mode can be prevented if the size of the transverse frames is ensured to be adequate.

2.2.1. Overview of previously established methods

Several attempts to capture how a stiffened panel contributes to the overall strength of the hull girder have been made since the 1960's. Caldwell [15] and later Faulkner [16] worked on a method to calculate the ultimate moment of a midship section, considering an instability strength reduction factor for compressed structures. An engineering approach was considered by Billingsley [17], when each beam-column element was modelled individually, with the strength of the hull girder being obtained from the summation of each contribution. These approaches based their predictions on the collapse strength of an individual plate, while subsequent methods such as Adamchak [18] and Lin [19] considered the sequence of collapsing plates.

Incredibly significant results were drawn by Rutherford and Caldwell [20], when analysing a specific case study where a Very Large Crude Carrier broke. The comparison between the ultimate bending moment experienced by the vessel under analysis and the theoretical predictions of the ultimate longitudinal bending strength of the hull considering a simplified approach, allowed to validate the considered model.

2.2.2. Method for the strength of thin stiffened plates

The method proposed by Gordo & Guedes Soares [21] consisted in the production of load shortening curves for stiffened plates based on mathematical expressions which had been proved to be appropriate for design purposes. This method assumes that the considered materials present an elastic-perfectly plastic behaviour, neglecting the change in the tangent modulus beyond the proportional stress and the hardening after yielding. This approximation is accurate for most structural steels, as the strains attained until collapse will never surpass three or four times the yield strain.

The compressive strength of a plate depends on its geometry and mechanical properties, namely on its slenderness - β – which translates the geometrical relation between the plate's width, thickness and yield strain.

A typical approach to deal with the reduced strength of the plates is by equating it to the strength of a plate with an effective width Φ_w, that collapses at nominal yield stress. Consequently, referring to effective width or to ultimate strength becomes equivalent.

Faulkner et al [22] established a model based on the Johnson-Ostenfeld formulation for the ultimate strength of thin stiffened plates where both the stiffener and an effective strip of the plate are subjected to an edge stress.

The average stress of a column under its yield strain, consists of a weighted average considering both stiffener and plate area contributions (considering effective plate width) to the column stress. Since this average stress is evaluated at yield strain, it actually translates the compressive strength of the stiffened plate column.

The different panel failure modes presented in Chapter 2.2 are modelled using slightly different mathematical formulations. Effectively, and considering a more detailed approach, the compressive strength of the stiffened plate column is given by the minimum of two functions, one representing the strength due to flexural buckling (equivalent to the expression denoted by Equation [19]), and one due to tripping of the stiffener. However, tripping of stiffeners is frequently dismissed, based on the assumption of strong stiffener torsional rigidity. Besides, one must consider that this approach assumes small initial deformations and absence of load eccentricity. An allowance for the effect of residual stresses on the plate strength has already been developed and can be taken into account, while considering residual stresses of the stiffener would be considered an improvement.

2.3. Local strength assessment of secondary structure

In the present chapter, another important component of the database analysis will be introduced: the local strength assessment of secondary structure. Unlike the previously addressed variable, the stiffened panel strength, which assessed how each panel element contributed to the overall midship section strength [15], this entity evaluates how stiffened panels respond under local lateral pressures.

This assessment is carried out using a simple mechanics of materials approach. The stiffened panel element is modelled as a beam, simply supported on its ends (corresponding to the length between consecutive frames) and subjected to a uniformly distributed load, which represents the applied local lateral pressure. Then, and knowing the bending moment distribution, it becomes possible to assess the maximum bending stress depending on the applied lateral pressure.

Since this local strength assessment considers a load applied along the stiffened panel, while the stiffened panel strength evaluates the panel contribution to the midship section strength when withstanding hull girder loads, it is clear that these methods will certainly impact the ship design procedure differently.

For larger vessels, where the more significant loads are due to the balancing of longitudinal weight and buoyancy distributions, the stiffened panel strength is the defining design variable. On the other hand,

smaller vessels are more drastically influenced by local loads, namely regarding lateral pressure. Considering this aspect, it is expected to find visible differences between the local strength assessment for smaller and larger vessels. The local strength assessment for smaller vessels is likely to present a dependence on ship length and no dependence whatsoever for larger vessels.

2.4. Shipbuilding industry overview

2.4.1. Developments in the shipbuilding industry

The international competition, namely from Far-East shipbuilding companies, that has been experienced by the European shipbuilding industry in the last decades, has seriously influenced new ship orders. This phenomenon led to studies regarding the feasibility of new technologies and methods in the production process, namely regarding the improvement in both cutting and welding technologies, as referred by Gordo et al. [23].

The Lean methodology, developed by Japan after the 2nd World War, and frequently referred to as the Toyota Production System (TPS), emerged as a tool to identify and eliminate seven major wastes: overproduction, waiting, motion, transport, over processing, inventory and defects [24]. This methodology was imported to the shipbuilding industry during the 1990's, with the works of Storch and Lim [25] and Liker and Lamb [26] depicting how beneficial the implementation of the TPS was for the panel assembly line.

A production process must be fully understood and analysed to correctly budget a given work order. Only at that point can a shipyard make the best budget approach to remain relevant in an increasingly competitive shipbuilding market. Several attempts have been made throughout the years to accurately predict the decomposition of the ship's hull total cost into several smaller parts associated to a given cost. This thought process allows the shipyard to assess which of the shipbuilding stages need to be improved for a more efficient production.

A study to evaluate the implementation of different cutting and welding procedures to analyse the consequences on the variation of the production's time and cost parameters was carried out by Leal and Gordo [27]. Also, by implementing and developing simulation tools, other sets of studies were conducted to obtain a better understanding of the production flow when faced with different production options [28] [29].

2.4.2. Cost evaluation in the shipbuilding process

Many shipyards derive cost estimates based on the costs per ton or man-hours per ton, which are typically obtained from records of recent construction projects. However, there's been an increasing demand for more accurate methods, that consider specific features and cost items based on databases of vessels that are relevant to each newbuilding project.

Lin and Shaw [30] developed an innovative cost estimation method called the feature-based estimation, based on the preliminary specifications to estimate ship costs, including the steel, other main materials, engine, power generator, other core equipment and labour hours. This method establishes the topology of the relationships between the features by linking the general dimensional parameters and detailed features of the specifications of the designs and cost information to estimate the main cost items of the ship. This approach has proven to be adequate for modern ships, leading to errors of the estimated total costs of no more than $\pm$7%, as shown in Table 2.1.

Table 2.1. Estimation results (Source: Lin and Shaw [30])

Comparison of the estimation results

SHIP	A	B	C
Type	Feeder	Panamax	New Panamax
LPP [m]	169	246.4	352
Breadth [m]	27	37	51
Error (%) of Total Cost	0.84	-2.63	6.90
Error (%) of Material Cost	7.30	-8.44	11.72
Error (%) of Labour Cost	0.61	2.95	-25.70
Error (%) of Overhead Cost	-6.38	-2.55	27.31

The error differences are calculated as follows:
(the estimated cost – the real cost)/the real cost x 100%

3. Implementation of formulations

This chapter will present all the practical aspects regarding the implementation of the stiffened panel strength, local strength assessment of secondary structure and production costs formulations, explaining all the assumptions made for a general case study.

The ship database will be introduced, namely regarding the different types of ships and the range of ship dimensions considered. Afterwards, all the specific geometrical aspects of typical stiffened ship panels will be introduced as the defining variables for both the stiffened panel strength and production costs computations.

3.1. Ships database

In order to significantly represent the shipbuilding industry worldwide, the established database comprises data collected from the midship section drawings of 15 ships built in shipyards from across the globe. Besides, the incorporation of ships built across a 50-year period allows for an interesting study regarding not only how the panel strength and cost is influenced by geometrical aspects, but also how the evolution of the ship design and shipbuilding industry through time has influenced these aspects.

For each of the entries of the ship database, the following data (considered as essential for the sake of the study) was gathered:

- Ship type
- Length between perpendiculars (LPP)
- Breadth
- Scantling draught
- Web frame spacing (l)

In cases where additional information was available, entities such as the built year, moulded depth, double bottom height and longitudinal bulkhead location (the transverse distance between the longitudinal bulkhead and the centreline) were also given as an input to the respective entry. The situations where these parameters were not gathered have to do with either the inexistence of such specification in the provided midship section drawings, or with the fact that such parameters do not apply to the considered ship structural design. For instance, several structural designs for bulk carriers do not present a longitudinal bulkhead, hence the absence of its location in certain database entries.

The gathered database presents a wide and varied scope of vessels that depict the shipbuilding market over the last decades in a representative way. With an even distribution regarding both the ship types

and ship lengths (as depicted in Table 3.1 and Table 3.2, respectively), it becomes possible not only to assess global tendencies in terms of panel strength and production costs, but to extend this type of analysis to a more detailed level, focusing on trends evidenced by each individual ship type.

Table 3.1. Ships database composition in ship types

Ship type	Number of database entries
Bulk carrier	3
Container carrier	2
Multipurpose vessel	3
Passenger ship	4
Tanker	3

Table 3.2. Ships database composition in LPP [m]

LPP [m]	Number of database entries
73 – 114	4
114 – 155	3
155 – 196	1
196 – 238	2
238 – 279	3
279 – 320	2

3.2. Ship panels database

A subsequent database was defined to comprise all the information regarding every individual stiffened panel found in each of the entries of the ships database. Once again, the data from the detailed midship section drawings was gathered to represent the generality of each ship's structural design. Keeping this objective in mind, and since most designs present several panel arrangements in each structural area, the most frequent stiffened panel in each area was inputted into the database as being the most representative panel of the specified structural area.

To keep a consistent pattern when inputting the stiffened panel data in the database, the only structural areas considered were the bottom, deck, double bottom, longitudinal bulkhead, and side shell areas. In certain areas, multiple panels per structural area were added to the database for the same ship entry. In some cases this was done for structural areas such as the deck, longitudinal bulkhead, and side shell areas. With respect to the deck structural area, it is of common knowledge that particularly in passenger ships such as cruise ships there are multiple decks in the arrangement of the ship structure. For this reason, it was decided to include each of the existent deck areas in the panel database, individually. In a similar manner, multiple panels associated with either the longitudinal bulkhead or side shell areas of the same ship were added to the panel database as individual entries. This decision was based on the

fact that the defining structural characteristics of these areas tend to present significant differences depending on whether the bottom, middle or top sections of these areas are considered.

Considering the typical arrangement of a general stiffened panel (consisting of longitudinal stiffeners and the respective attached steel plating), the following essential data was gathered for the ship panel database:

- Panel type
- Location (when applicable)
- Longitudinal stiffener spacing
- Plate thickness
- Plate material
- Stiffener type (flat bar, bulb, angle, or T cross-sections)
- Stiffener web height
- Stiffener flange width (when applicable)
- Stiffener web thickness
- Stiffener flange thickness (when applicable)
- Stiffener material

The composition of the ship panels database regarding the considered panel types is displayed in Table 3.3, showing a good representation of every type of panel. This will allow for one not only to evaluate overall tendencies regarding the ship panels strength and production costs, but to look with further detail to the specific trends regarding each individual panel type, facilitating a comparative study between them. The higher number of longitudinal bulkhead or side shell panels is, as previously stated, a consequence of the significant structural differences between the top, middle or bottom portions of these areas in each vessel.

Figure 3.1 depicts a standard midship section configuration of a cargo vessel, in this specific case, of a tanker vessel. The several different types of ship panels considered in this study are easily identifiable: bottom (1), double bottom (2), side shell (3), longitudinal bulkhead (4) and deck (5) panels.

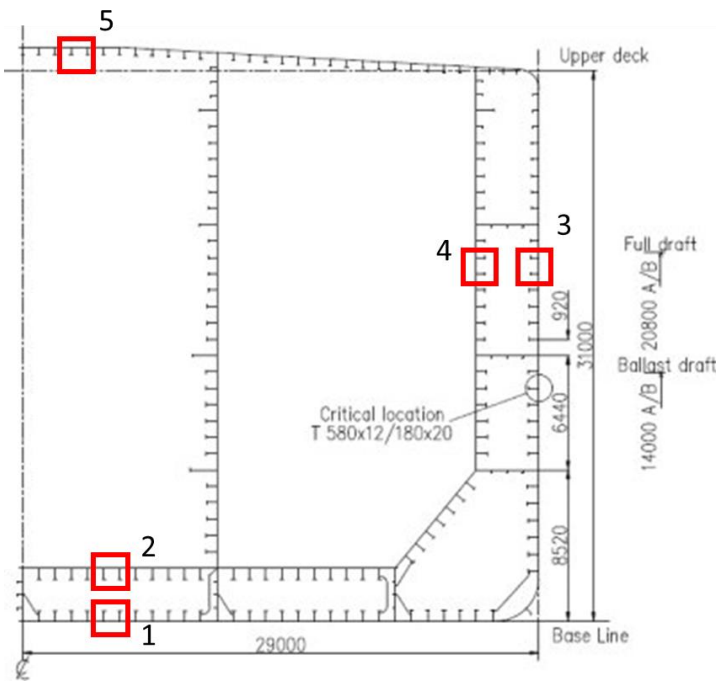

Figure 3.1. Typical midship section configuration and representative panel types (Source: Guedes Soares et al. [31])

Table 3.3. Ship panels database composition in panel types

Panel type	Number of database entries
Bottom	15
Deck	22
Double bottom	15
Longitudinal bulkhead	25
Side shell	30

The representation of how each entry in the ships database is associated with a given amount of ship panels database entries is depicted in Figure 3.2.

Ship ID	Ship type	LPP [m]	(...)	l [mm]
1	Tanker	134	(...)	3120
(...)	(...)	(...)	(...)	(...)
n	Multipurpose	112	(...)	3200

Ship ID	Panel ID	Panel type	(...)	Stiff. material
1	1	Bottom	(...)	A
(...)	(...)	(...)	(...)	(...)
1	n	Deck	(...)	A

Ship ID	Panel ID	Panel type	(...)	Stiff. material
n	1	Bottom	(...)	AH32
(...)	(...)	(...)	(...)	(...)
n	n	Long. Bulkhead	(...)	DH32

Figure 3.2. Integration of ships database (left hand side) and ship panels database (right hand side)

For instance, if the considered ships database consists of n ships, and each of the ships presents m significant panels, the ship panels database will be constituted by $n \times m$ entries. The mentioned scheme only translates the global relation between both databases, not actually presenting each of the fields which were gathered according with was defined in previous chapters.

3.3. Geometrical definition of a general stiffened panel

The present chapter will describe the geometrical characteristics gathered from a general stiffened panel. Later on, this will allow to estimate the strength of each entry in the ship panels database using the method described with detail in Chapter 2.2.2. A general stiffened panel is constituted by two main entities: a steel plate and a longitudinal stiffener which acts as a reinforcement. Each of these two entities are characterized by a set of geometrical and mechanical aspects that define the overall panel strength.

3.3.1. Characteristics of the components of a general stiffened panel

An example of a typical stiffened panel cross-section is shown in Figure 3.3. The two main geometrical aspects that define the plating are the plate thickness, t_p, and the plate breadth, b. The plate breadth is defined as the transverse distance between two consecutive longitudinal stiffeners. The plating material is usually characterized by its Young's modulus, E, and yield stress, σ_0.

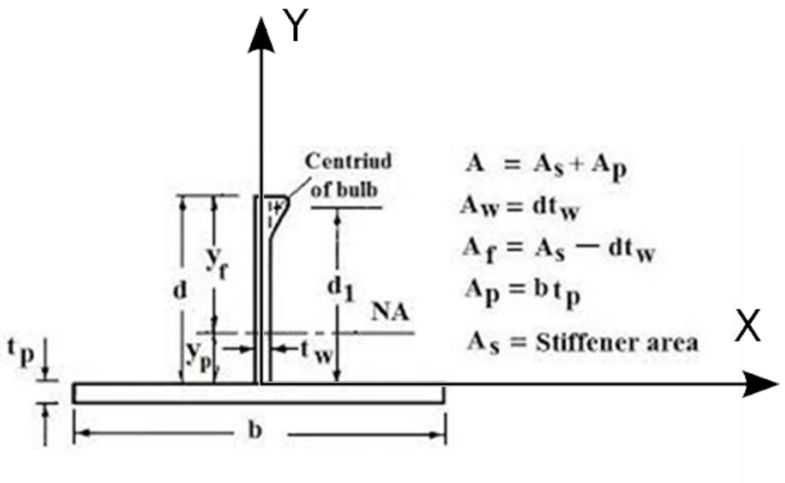

Figure 3.3. Geometric definition of a stiffened panel (bulb cross-section)

For the sake of this study, four types of stiffener cross-sections will be considered and described accordingly with Figure 3.4: flat bar, bulb, angle, and T cross-sections. Flat bars are characterized by web height, d_w, and web thickness, t_w. Bulb cross-section stiffeners are also characterized by web height, d_w, and web thickness, t_w, with the flange being fully defined according to general manufacture

standards depending on both the web height and thickness. Angle and T cross-section stiffeners are characterized by web height, d_w, web thickness, t_w, flange breadth, b_f, and flange thickness, t_f. Besides, and in the same way as the plating, the stiffener material is characterized by both the Young's modulus and the yield stress.

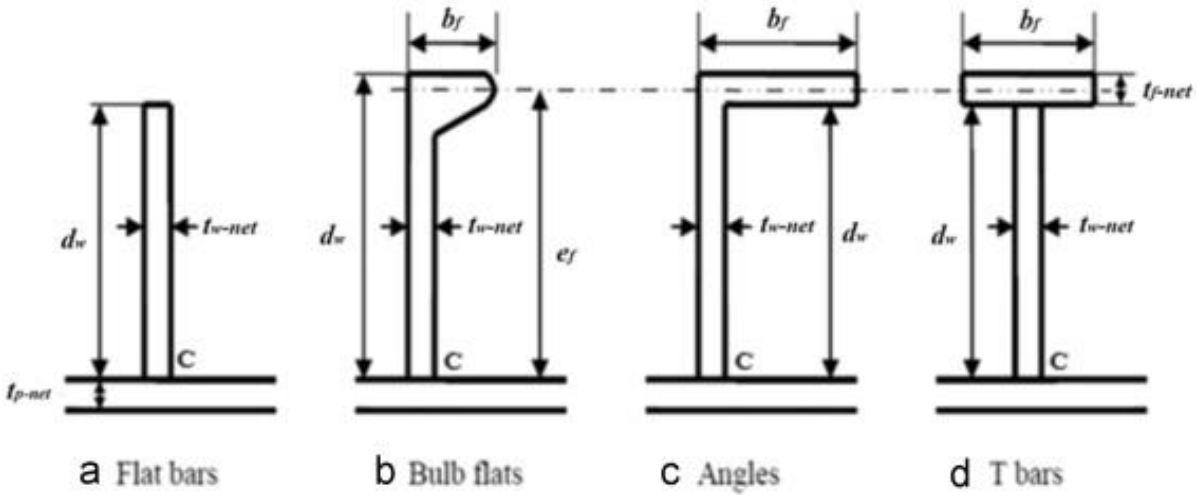

Figure 3.4. Geometric definition of several stiffener cross-sections

3.3.2. Cross-section properties of a general stiffened panel

The cross-section properties of a typical stiffened panel can be derived from simple equations using the entities presented in Chapter 3.3.1, and considering a coordinates system in accordance with the one presented in Figure 3.3. The following procedures led to the computation of the second moment of area about the x-axis, I_{xx}, which will be necessary to evaluate the radius of gyration of the cross-section of the column.

The vertical centre of gravity of the plate component, Y_{cg_p}, and the second moment of area about the x-axis of the plate component, I_{xx_p}, are defined in Equation [1] and Equation [2], respectively.

$$Y_{cg_p} = -\frac{t_p}{2} \quad [1]$$

$$I_{xx_p} = \frac{1}{12} b \cdot t_p^3 \quad [2]$$

The defining equations for the cross-section properties of the stiffener component depend on the considered cross-section. For bulb cross-sections, the vertical centre of gravity, second moment of area and cross-section area are all defined as a function of web height and thickness, being directly inputted from a manufacturer's catalogue. For flat bar, angle and T cross-sections, the cross-section area, A_s,

the vertical centre of gravity of the stiffener component, Y_{cg_s} and the second moment of area about the x-axis of the stiffener component, I_{xx_s}, are defined in accordance with Equation [3], Equation [4] and Equation [5], respectively.

$$A_s = \begin{cases} d_w \cdot t_w, & Flat\ bar \\ (d_w - t_f) \cdot t_w + b_f \cdot t_f, & Angle\ and\ T \end{cases} \quad [3]$$

$$Y_{cg_s} = \begin{cases} \frac{d_w}{2}, & Flat\ bar \\ \frac{\frac{(d_w - t_f)^2}{2} \cdot t_w + \left(d_w - \frac{t_f}{2}\right) \cdot b_f \cdot t_f}{A_s}, & Angle\ and\ T \end{cases} \quad [4]$$

$$I_{xx_s} = \begin{cases} \frac{1}{12} t_w \cdot d_w^3, & Flat\ bar \\ \frac{1}{12} t_w \cdot (d_w - t_f)^3 + \left(Y_{cg_s} - \frac{d_w - t_f}{2}\right)^2 \cdot t_w \cdot (d_w - t_f) + & \\ \frac{1}{12} b_f \cdot t_f^3 + \left(Y_{cg_s} - d_w + \frac{t_f}{2}\right)^2 \cdot t_f \cdot b_f, & Angle\ and\ T \end{cases} \quad [5]$$

Afterwards, the vertical centre of gravity of the column, Y_{cg_c}, can be evaluated using Equation [6].

$$Y_{cg_c} = \frac{Y_{cg_s} \cdot A_s + Y_{cg_p} \cdot b \cdot t_p}{A_s + b \cdot t_p} \quad [6]$$

Besides, the distance between the vertical centre of gravity of the plate and the centre of gravity of the column, d_p, and the distance between the vertical centre of gravity of the stiffener and the centre of gravity of the column, d_s, are both computed with Equations [7] and [8], respectively.

$$d_p = Y_{cg_p} - Y_{cg_c} \quad [7]$$

$$d_s = Y_{cg_s} - Y_{cg_c} \quad [8]$$

These distances will be used in Equation [9], to finally calculate the total second moment of area of the column cross-section, I_{xx}.

$$I_{xx} = I_{xx_s} + A_s \cdot d_s^2 + I_{xx_p} + b \cdot t_p \cdot d_p^2 \quad [9]$$

3.4. Implementation of stiffened panels strength formulations

In the present chapter, the major practical aspects regarding the step-by-step implementation of the method described in Chapter 2.2.2 will be presented and described. The equations presented throughout this chapter were then evaluated using as input the data gathered in both the ships and ship panels databases.

In accordance with what had been stated previously, the method for the computation of stiffened panel strength assumes an elastic-perfectly plastic behaviour of the considered materials.

$$\Phi(\bar{\varepsilon}) = \Phi_e = \begin{cases} -1, & \bar{\varepsilon} < -1 \\ \bar{\varepsilon}, & -1 < \bar{\varepsilon} < 1 \\ 1, & \bar{\varepsilon} > 1 \end{cases} \quad [10]$$

Equation [10] depicts how this behaviour is analytically represented. Φ_e is the edge stress ratio, i.e. the ratio between edge and yield stress, and $\bar{\varepsilon}$ is the average strain ratio, i.e. the ratio between edge and yield strain, ε_0. Afterwards, it becomes necessary to define of the most crucial aspects regarding plate compressive strength: plate slenderness, β.

$$\beta = \frac{b}{t_p} \cdot \sqrt{\varepsilon_0} \quad [11]$$

In Equation [11], b is the plate breadth and t_p is the plate thickness (according to what was defined in Chapter 3.3). For the sake of this study, the yield point will be considered. Next, the effective width of the plate, Φ_w, is defined.

$$\Phi_w = \frac{2}{\beta} - \frac{1}{\beta^2}, \qquad \beta > 1 \quad [12]$$

Equation [12] depicts how, for a given plate, the effective width goes from a value close to 1 to lower values, as the loading (and consequently the strain) is increasing. The normalised average stress of the plate, Φ_a, is obtained by the product of edge stress (Equation [10]) and the corresponding effective width (Equation [12]), as shown in Equation [13].

$$\Phi_a = \Phi_e \cdot \Phi_w \quad [13]$$

Later, it becomes necessary to define the Euler stress ratio, Φ_E, using Equation [14]. This ratio is defined as a function of the column slenderness, λ, which is defined in Equation [15].

$$\Phi_E = \left(\frac{\pi}{\lambda}\right)^2 \quad [14]$$

$$\lambda = \frac{l}{r}\sqrt{\varepsilon_0} \quad [15]$$

In Equation [15], l translates, once again, the length between frames and r translates the radius of gyration of the cross-section of the column, which can be evaluated using Equation [16]. Here, I_{xx} is the second moment of area about the x-axis and A_s is the cross-section area of the stiffener (variables previously established in Chapter 3.3).

$$r = \sqrt{\frac{I_{xx}}{A_s + b \cdot t_p}} \quad [16]$$

$$\Phi_E(\bar{\varepsilon}) = \frac{\Phi_E}{\bar{\varepsilon}} \quad [17]$$

Replacing the yield strain by a given strain in Equation [14], the Euler stress ratio can eventually be computed instantaneously using Equation [17].

$$\Phi_{\text{jo}} = \begin{cases} \Phi_E \cdot \Phi_e, & \Phi_E < 0.5 \\ \left(1 - \frac{1}{4 \cdot \Phi_E}\right) \cdot \Phi_e, & \Phi_E > 0.5 \end{cases} \quad [18]$$

The Johnson-Ostenfeld contribution for the average stress of a column, Φ_{jo}, is then evaluated using Equation [18].

Finally, the expression to calculate the average stress of a column under its yield strain, ε_0, and hence the compressive strength of a stiffened plate column, is obtained and presented in Equation [19].

$$\Phi_{\text{ab}} = \Phi_{\text{jo}} \cdot \frac{\frac{A_s}{b \cdot t_p} + \Phi_w}{\frac{A_s}{b \cdot t_p} + 1} \quad [19]$$

3.4.1. Corrosion additions and stiffened panel strength

An additional study will be carried out, concerning the influence of the corrosion additions on the stiffened panel strength. The corrosion additions are, in accordance with the Common Structural Rules

from IACS [32], the predicted thickness diminution due to corrosive effects. These additions are defined depending on the location of the considered panel or stiffener.

$$t_c = Roundup_{0.5}(t_{c1} + t_{c2}) + t_{res} \quad [20]$$

Equation [20] presents the formula to compute the total corrosion addition, in mm, t_c, where $Roundup_{0.5}$ translates the rounding to the upper half millimetre. The values for t_{c1} and t_{c2} correspond to corrosion additions for each of the sides of the considered structural member and t_{res} is the reserve thickness, taken as 0.5 mm.

For the sake of this study and keeping in mind the arrangement shown in Figure 3.1, t_{c1} was considered for the outer side of bottom and side shell panels, for the inside of double bottom and longitudinal bulkhead panels and for the upper side of deck panels. Correspondingly, t_{c2} was considered for the opposite side of each panel. The overall corrosion additions for each of the considered panel types are presented in Table 3.4 and Table 3.5.

Table 3.4. t_{c1} corrosion additions

$t_{c1}\ [mm]$	Bulk carrier	Container carrier	Multipurpose	Passenger	Tanker
Bottom	1	1	1	1	1
Double bottom	2.4	0.5	2.4	0.5	2.1
Side shell	1	1	1	1	1
Long. Bulkhead	1.2	1	1.2	1	1
Deck	1	1	1	1	1

Table 3.5. t_{c2} corrosion additions

$t_{c2}\ [mm]$	Bulk carrier	Container carrier	Multipurpose	Passenger	Tanker
Bottom	1.7	1.7	1.7	1.7	1.7
Double bottom	1.7	1.7	1.7	1.7	1.7
Side shell	1.2	1.2	1.2	1.2	1.2
Long. Bulkhead	1.2	1.2	1.2	1.2	1.2
Deck	0.5	0.5	0.5	0.5	0.5

With respect to the stiffener thicknesses, the corrosion additions were composed by $2t_{c2}$, as this corresponds to the side of the panel where the connection between stiffener and plate is located.

To assess the influence of the corrosion additions on the stiffened panel strength results, the corrosion additions regarding each panel will be computed (both plate and stiffener elements). Afterwards, they will be deducted from the original thicknesses to compute the stiffened panel strength, using the

formulations defined in Chapter 3.4. These values will then be compared to the results previously obtained, when considering the original thicknesses.

3.5. Implementation of the local strength assessment of secondary structure

In the present chapter, the implementation of the local strength assessment procedure will be explained in detail. The formulations presented in the present chapter reflect the introduction to bending stress due to local loads given in Chapter 2.3.

First, the mechanics of materials approach used to model the panel structure will be dealt with, deducting the relevant expressions from classic formulations and justifying the assumptions made throughout the process. Additionally, the attained expression for the local strength assessment and the Common Structural Rules for Bulk Carriers and Oil Tankers [32] expression for the minimum net section modulus for applicable design loads will be related and compared. Furthermore, the significant differences between stiffened panel strength and local strength assessment and the respective expected influence on the obtained results, will be discussed.

3.5.1. Mechanics of materials approach

The mechanics of materials approach that enables the local strength assessment of the secondary structure is based on the analogy between a simply supported beam subjected to uniformly distributed load (Figure 3.5) and a stiffened panel subjected to a local lateral pressure.

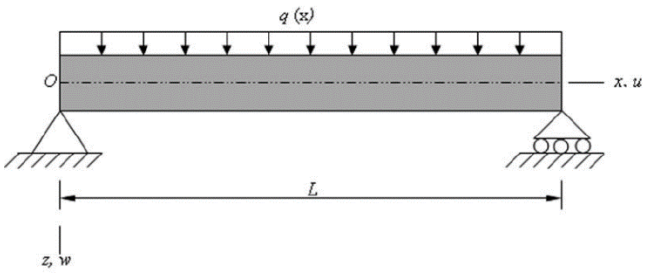

Figure 3.5. Simply supported beam subjected to uniformly distributed load

Regarding the scheme presented in Figure 3.5, the simply supported ends of the beam can be compared to the web frame ends of a stiffened panel, hence the beam length, L, is evaluated as the length between frames, l, using this approach. Besides, the uniformly distributed load q, can be similarly represented by the product between the longitudinal stiffener spacing, s, and the local lateral pressure, p. It was considered that the web frames limiting the stiffened panels wouldn't contribute to any restriction

regarding the rotation of the panels ends, hence the assumption of simply supported beam ends, instead of clamped or fixed ends.

The first step in this procedure is presented in Equation [31], which translates the static moment equilibrium equation at point x=0 (one of the beam ends), considering a reaction force, $R_{x=0}$, at this point.

$$\sum M_{x=l} = 0 <=> R_{x=0} \cdot l - p \cdot s \cdot l \cdot \frac{l}{2} = 0 \quad [21]$$

Considering the uniform distribution of the load applied on the beam, it's instinctive to assess that the reaction forces at both beam ends are equal to the same value, as expressed in Equation [22].

$$R_{x=0} = R_{x=l} = p \cdot s \cdot \frac{l}{2} \quad [22]$$

Then, and considering the reaction force at the beam end and the uniformly distributed load, it is possible to establish an expression to evaluate the shear force at any point along the beam, using Equation [23]. This expression translates a linear variation of shear force along the beam, with a zero at x=$\frac{l}{2}$ (half of the span of the beam).

$$V(x) = R_{x=0} - p \cdot s \cdot x = p \cdot s \cdot \left(\frac{l}{2} - x\right) \quad [23]$$

Correspondingly, the expression for the bending moment along the beam is determined in Equation [24]. This expression shows a parabolic behaviour, with a maximum bending moment occurring at x=$\frac{l}{2}$, and zero bending moment at the simply supported beam ends (x=0 and x=l).

$$M(x) = R_{x=0} \cdot x - p \cdot s \cdot x \cdot \frac{x}{2} = \frac{p \cdot s \cdot x}{2} \cdot (l - x) \quad [24]$$

$$M_{max} = M\left(x = \frac{l}{2}\right) = \frac{p \cdot s \cdot l^2}{8} \quad [25]$$

Then, it becomes possible to define the expression for the maximum bending stress, $\sigma_{x\,max}$:

$$\sigma_{x\,max} = \frac{M_{max} \cdot c}{I_{xx}} = \frac{p \cdot s \cdot l^2}{8} \cdot \frac{c}{I_{xx}} \quad [26]$$

Where c denotes the neutral axis position, which in this case equals the vertical centre of gravity of the beam cross section, Y_{cg_c}, previously defined in Equation [6].

To present results without having to assume lateral pressure values, the present study will focus on two distinct variations of the maximum bending stress expression shown in Equation [26].

$$\frac{\sigma_{x\,max}}{p} = \frac{s \cdot l^2 \cdot c}{8 \cdot I_{xx}} \quad [27]$$

$$p = \frac{8 \cdot I_{xx} \cdot \sigma_0}{s \cdot l^2 \cdot c} \quad [28]$$

The first one, shown in Equation [27], presents the ratio between maximum bending stress and lateral pressure, leading to the evaluation of the magnitude of the attained maximum bending stress for a unity of lateral pressure. The second one, shown in Equation [28], presents the lateral pressure value at which the attained maximum bending stress equals the yield stress.

The two variations will present opposite behaviours. One could immediately deduct this from a mathematical standpoint, as for instance Equation [28] is simply the inverse of Equation [27] multiplied by the yield stress, σ_0. Nonetheless, a simple principle is behind this reasoning: if a given panel A presents a higher maximum bending stress over lateral pressure than panel B, this same panel A will correspondingly require a lower lateral pressure than panel B to reach the bending yield stress.

The derived expression for the maximum bending stress - Equation [26] - can be rearranged in a way to isolate the section modulus, Z, which is given by the ratio between I_{xx} and c.

$$Z = \frac{p \cdot s \cdot l^2}{8 \cdot \sigma_{x\,max}} \quad [29]$$

Equation [29] can be compared to the minimum stiffener net section modulus expression defined in Ch. 6, Sec. 5 of the Common Structural Rules for Bulk Carriers and Oil Tankers [32], presented in Equation [30].

$$Z = \frac{|P| \cdot s \cdot {l_{bdg}}^2}{f_{bdg} \cdot \chi \cdot C_S \cdot R_{eH}} \quad [30]$$

Where $|P|$ is the absolute value of the design pressure, s is the stiffener spacing, l_{bdg} is the effective bending span, f_{bdg} is a bending moment factor, χ is a coefficient to account for either intact or flooded conditions, C_S is the permissible bending stress coefficient and R_{eH} is the specified minimum yield stress.

3.5.2. Comparative analysis of stiffened panel strength and local strength assessment

Significant differences are expected regarding the results for both stiffened panel strength and local strength assessment. The stiffened panel strength results translate how effective is the contribution of each of the stiffened panel elements to the overall midship section strength, which allows to assess how much of the bending moment (hog and sag) the vessel can tolerate. On the other hand, the local strength assessment using the mechanics of materials approach previously described, allows to evaluate the maximum bending stress caused by a local lateral pressure along a stiffened panel.

Considering the global (stiffened panel strength) and local (local strength assessment) character of these two approaches, it becomes logical that their relative importance to the design process is also dependent on the considered situation. For smaller sized vessels (for instance, with LPP lower than 150 m) the local approach will become more significant, while for larger vessels the global approach considering longitudinal bending will be driving the design process.

Keeping this dichotomy in mind, it is expected to find more significant variations in the amount of structural material allocated to distinct panel types for larger vessels, where the stiffened panel strength is expected to be the defining variable. These variations will have to do with the distance from each of the considered panel types to the neutral axis of the midship section. Panels located further away from the neutral axis, such as bottom and double bottom panels, will have to withstand higher bending stresses. Consequently, a higher amount of structural material is required in these areas, leading to higher stiffened panel strength values.

3.5.3. Corrosion additions and local strength assessment

The influence of corrosion additions on the local strength assessment of secondary structure was also studied. Following the procedure described in Chapter 3.4.1, the predicted thickness diminution due to corrosive effects in mm, t_c, is computed in accordance with the Common Structural Rules from IACS [32].

Table 3.4 and Table 3.5 resume all the information regarding the overall corrosion additions for each of the considered panel types. Once again, in accordance with Chapter 3.4.1, the corrosion additions for stiffeners were composed by $2t_{c2}$, as this relates to the side of the panel where the stiffener and the plate are connected.

To evaluate the influence of the corrosion additions on the local strength assessment results, it is required to deduct the corrosion additions from the original plate and stiffener thicknesses. These

resultant thicknesses will then be used for the local strength assessment procedure defined in Chapter 3.5.1. These values will then be compared to the results obtained when considering the original thicknesses.

3.6. Implementation of production costs formulations

The practical aspects considered in the computations of each individual contribution to the overall production cost of a stiffened panel will be presented and discussed in the present section. For the sake of this study, material, cutting, assembly and welding costs were considered as the defining components to the overall production costs for standard stiffened panel shipbuilding. Further level of detail could have been introduced by contemplating other components, such as transportation and painting cost estimates.

Furthermore, specific methods were considered for each shipbuilding stage, namely plasma cutting for all cutting procedures and submerged arc welding for all welding procedures. These procedures were adopted as they are representative of a large portion of the used methods in shipbuilding around the globe and to ensure a common comparative basis between all the regarded panels.

3.6.1. Material costs

The material costs were considered as the simple acquisition costs for the steel plates and stiffeners. To evaluate this, and since the vast majority of this market regards prices per unit weight of steel, the first step was to calculate the plate and stiffener weights.

Equation [31] depicts the calculation of the weight of a panel of width w_p and length corresponding to the web frame spacing. The considered panel width is obtained by computing the round-up to the closest integer of the ratio between 2000 mm and the longitudinal stiffener spacing, s, and then multiplying this factor by the longitudinal stiffener spacing, leading to panel widths between 2000 and 3500 mm. The steel density, ρ_{steel}, is considered as 7.85 t/m^3.

$$W_p = w_p \cdot t_p \cdot l \cdot 10^{-9} \cdot \rho_{steel} \quad [31]$$

In a similar manner, the weight of the panel stiffeners is evaluated using Equation [32]. It is noticeable how the factor $\frac{w_p}{s}$ accounts for the number of stiffeners present in each panel.

$$W_s = \frac{w_p}{s} \cdot A_s \cdot l \cdot 10^{-9} \cdot \rho_{steel} \quad [32]$$

Finally, and considering 600 €/t and 412 €/t as the plate and stiffener prices per unit weight, respectively, the total material costs, C_m, were evaluated using Equation [33].

$$C_m = 600 \cdot W_p + 412 \cdot W_s \quad [33]$$

3.6.2. Cutting costs

The cutting costs regarded for this study comprise two main components: operational cutting costs and electricity costs. The operational costs are the result of a deduction made in the work of Leal and Gordo [27], where shipyard estimated costs of 150 €/t of steel were considered. In this case, the steel weight is composed of the plate weight, W_p, and the stiffeners weight, W_s.

The electricity costs account for an estimated plasma cutting power of 55 kW at a price of 0.10 €/kWh. The electricity consumption can be estimated using the cutting time, which needs to be evaluated using an assumed plasma cutting speed of 99.5 m/h and the cutting length, l_c. The cutting length for standard stiffened panels considers the contributions of both the plate and the stiffeners, as expressed in Equation [34].

$$l_c = 2 \cdot \left(w_p + l + \frac{w_p}{s} \cdot d_w\right) \cdot 10^{-3} \quad [34]$$

The total cutting costs are then evaluated using Equation [35], which includes all the previously referred assumptions regarding the cutting process.

$$C_c = 150 \cdot \left(W_p + W_s\right) + 0.10 \cdot 55 \cdot \frac{l_c}{99.5} \quad [35]$$

3.6.3. Assembly costs

The assembly costs translate the work force required to assemble the longitudinal stiffeners in their respective welding position. Leal and Gordo [27] estimated a work efficiency of around 0.56 man-hours per metre of longitudinal stiffener assembly, which combined with an assumed work cost of 8 € per man-hour, leads to an estimate of total assembly costs, C_a, as shown in Equation [36].

$$C_a = 8 \cdot \left(0.56 \cdot l \cdot 10^{-3} \cdot \frac{w_p}{s}\right) \quad [36]$$

3.6.4. Welding costs

The welding costs are computed based on the welding electrode consumption. To correctly estimate the consumption of the electrode, one must consider the differences between plate-plate welds (butt joints) and plate-stiffener welds (tee joints), regarding not only the cross section of the weld, but also how the type of joint influences the number of weld ropes required.

Figure 3.6 depicts the typical butt joint considered for this study. In accordance, the plate-plate weld cross section area, $A_{w_{pp}}$, is defined in Equation [37].

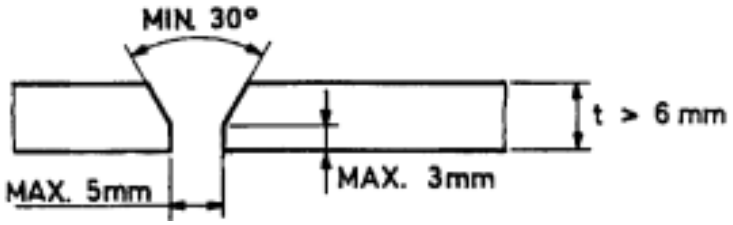

Figure 3.6. Butt joint geometrical definition (Source: DNV [33])

$$A_{w_{pp}} = 5 \cdot t_p + \left(t_p - 3\right)^2 \cdot \tan\left(\frac{30°}{2}\right) \quad [37]$$

The corresponding plate-plate weld length, $L_{w_{pp}}$, is presented in Equation [38]. Only half of the total perimeter of each individual panel is considered, as the remainder of the panel perimeter is welded in the following attached panel. This was done not to account for the same welds twice, which would result in an unrealistic estimation.

$$L_{w_{pp}} = w_p + l \quad [38]$$

On the other hand, a typical tee joint section consists of a rectangle triangle, with equal adjacent sides of the triangle. For the sake of this study, it was considered a triangle with adjacent sides equal to the stiffener web thickness, t_w, leading to a plate-stiffener weld cross section area, $A_{w_{ps}}$, as defined in Equation [39].

$$A_{w_{ps}} = \frac{t_w^2}{2} \quad [39]$$

The plate-stiffener weld length, $L_{w_{ps}}$, is presented in Equation [40], and depicts how two weld ropes (one in each side of each longitudinal stiffener) are required for a proper tee joint.

$$L_{w_{ps}} = 2 \cdot \frac{w_p}{s} \cdot l \quad [40]$$

The total weld weight (in kg) is then evaluated using Equation [41], multiplying the weld volume by the steel density.

$$W_w = \left(A_{w_{pp}} \cdot L_{w_{pp}} + A_{w_{ps}} \cdot L_{w_{ps}}\right) \cdot 10^{-6} \cdot \rho_{steel} \quad [41]$$

The total welding costs are then computed using Equation [42], and taking in consideration a price of 38 € for each 16 kg electrode reel, as estimated in Leal and Gordo [27].

$$C_w = 38 \cdot \frac{W_w}{16} \quad [42]$$

4. Presentation and discussion of results

The presented methods regarding panel strength assessment (Chapter 3.4), local strength assessment of secondary structure (Chapter 3.5) and production costs (Chapter 3.6) were applied to the gathered ship panel database. Afterwards, the attained results regarding panel strength, local strength assessment and production costs will be subjected to several parametric analyses in Chapter 4.1 Chapter 4.2 and Chapter 4.3, respectively.

This procedure aims at understanding eventual underlying relations between panel strength, local strength assessment and production costs, and geometric characteristics at a global (ship geometry) or local (panel geometry) level. In each of the following chapters, different studies were carried out depending on the analysed feature, as certain aspects are not equally influential for either panel strength, local strength assessment or production costs due to the major disparities between what these parameters stand for.

4.1. Stiffened panels strength results

In the present chapter, the results obtained regarding panel strength will be presented in two distinct approaches: as function of LPP and as function of panel aspect ratio (the ratio between panel length, which corresponds to the web frame spacing, and panel width). The choice of these two parameters has to do with, as previously pointed out, the attempt to establish relations between panel strength and both ship-level and panel-level variables.

From the many possible options regarding geometrical variables at ship-level, the LPP seemed to be the most defining, since this study only covers the longitudinal stiffening of ship panels, and the longitudinal strength is mostly influenced by the ship's length. At a panel-level, the aspect ratio between panel length and width seemed an interesting variable to discuss, as it allows for a consideration regarding not only the span of the stiffeners, but also their spacing and, consequently, the number of stiffeners contributing to the panel strength. It is also widely used for buckling studies regarding compressed stiffened panels, so it's only right to also assess its influence on stiffened panels strength.

4.1.1. Influence of ship length in panel strength

In this section, it is analysed and discussed the dependence of the compressive strength from the length of the ship, LPP, for different locations: bottom, double bottom, side shell, longitudinal bulkhead and deck panels. It presents the influence of overall ship parameters on the panel strength in different ship panels. Besides, it is assessed if there is any pattern regarding both ship type and panel type.

Figure 4.1 depicts different behaviours regarding the influence of LPP in bottom panel strength.

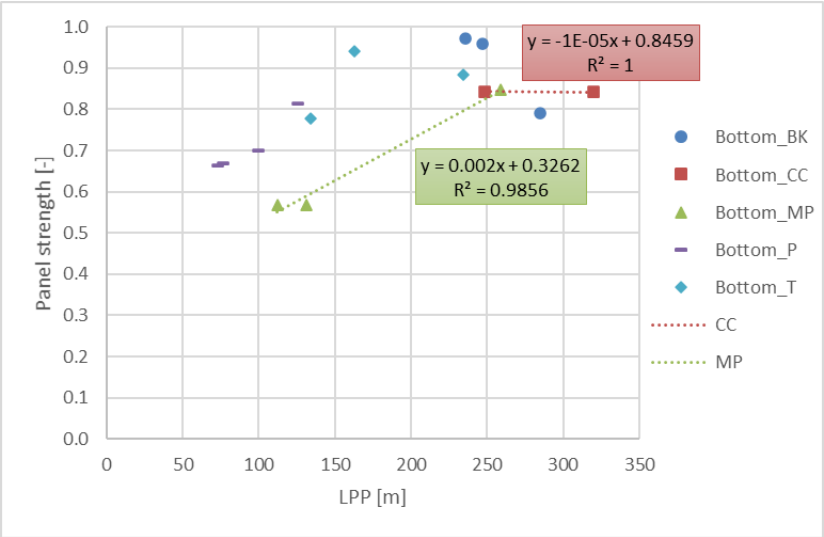

Figure 4.1. Bottom panel compressive strength as a function of LPP [m]

Overall, the bottom panel strength increases proportionally with LPP, until it reaches a sort of asymptote at about 0.9, for LPP values higher than 200 m.

For multipurpose, passenger and tanker vessels, an increase in bottom panel strength is verified when associated with larger LPP values, while for bulk carrier vessels the opposite occurs, as an increase in LPP translated into lower bottom panel strength values. Moreover, the bottom panel strength of container carrier vessels comes out as independent of LPP, with constant values all over the board.

The mentioned behaviours observed for both container carrier and multipurpose vessels are verified when evaluating the fitting line expressions and the coefficient of determination (R^2) presented in Figure 4.1. A proportional function for multipurpose vessels and an approximately constant expression for container carriers is depicted in the fitting line expressions presented in Equations [43] and [44], respectively.

$$Panel\ strength = 0.002 \times LPP + 0.326 \quad [43]$$

$$Panel\ strength = -10^{-5} \times LPP + 0.846 \quad [44]$$

Furthermore, the coefficient of determination (R^2), which assesses how suitable the fitting line is for the considered data, is close to 1 for both cases, ensuring an adequate fitting line.

Regarding double bottom panel strength, Figure 4.2 shows similar tendencies when comparing to the bottom panel strength results presented in Figure 4.1.

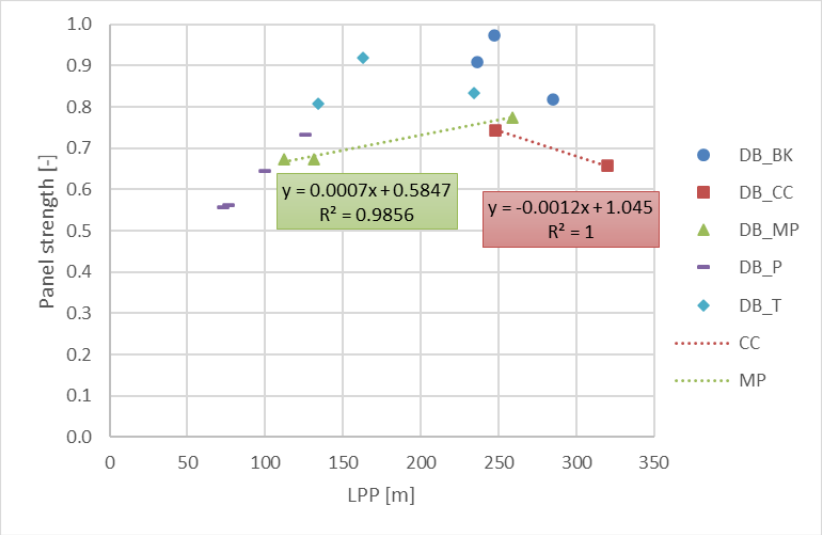

Figure 4.2. Double bottom panel compressive strength as a function of LPP [m]

This resemblance is mostly due to both bottom and double bottom panels presenting equal stiffener spacing and similar distances relatively to the midship section neutral axis, leading to comparable amounts of steel, and consequently similar panel strength tendencies. The global results show an increase of panel strength caused by the increase in LPP up to a certain point (once again at LPP values around 200 m), from whereout strength values stagnate and eventually decrease.

Multipurpose and passenger vessels show an increase in double bottom panel strength with higher LPP values, in the same manner as it occurred for bottom panels of this sort. Bulk and container carriers, however, present decreasing strength when associated with increasingly higher LPP. Once again, the behaviours observed for both container carrier and multipurpose vessels are verified when evaluating the fitting line expressions and the coefficient of determination (R^2) presented in Figure 4.2. The fitting line expressions depict a proportional function for multipurpose vessels (Equation [45]) and an inversely proportional expression for container carriers (Equation [46]). Besides, the coefficient of determination (R^2), is close to 1 for both cases, ensuring an adequate fitting line.

$$Panel\ strength = 0.0007 \times LPP + 0.585 \quad [45]$$

$$Panel\ strength = -0.0012 \times LPP + 1.05 \quad [46]$$

Tanker vessels show a maximum panel strength at an LPP value of a little over 150 m. Due to the short sample size of this type of panels, it can't be properly stated if this translates an actual parabolic behaviour (with the panel strength increasing up to a maximum and then descending with further increase in LPP), or if it's a simple deviation in an overall constant panel strength tendency.

Side shell panels results presented in Figure 4.3 exhibit a standard pattern in terms of panel strength for most ship types.

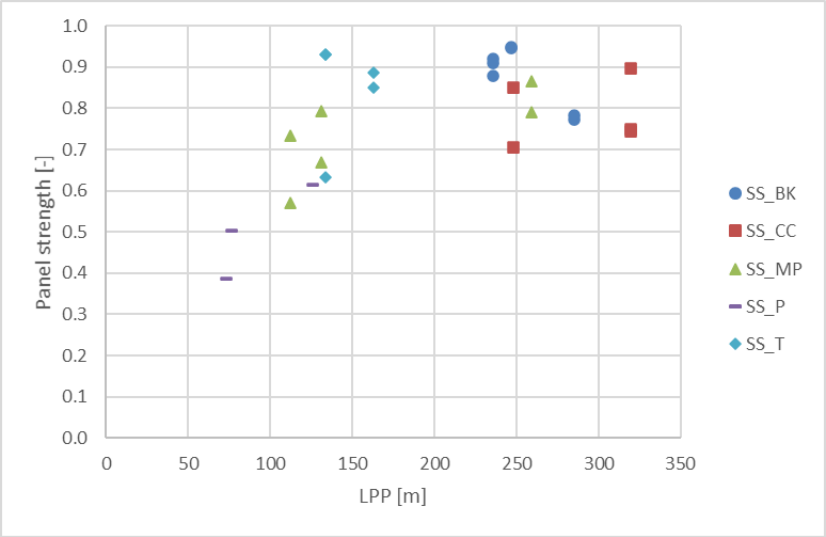

Figure 4.3. Side shell panel compressive strength as a function of LPP [m]

Figure 4.3 shows that except for bulk carriers, every other ship type presents an increasing side shell panel strength with increasing LPP. The global tendency that has been observed throughout this study is once again evident: panel strength increases until LPP values larger than 200 m are attained, from whereout an asymptotic value of 0.8 is observed.

Figure 4.4 shows the longitudinal bulkhead panel strength results assessed in this study.

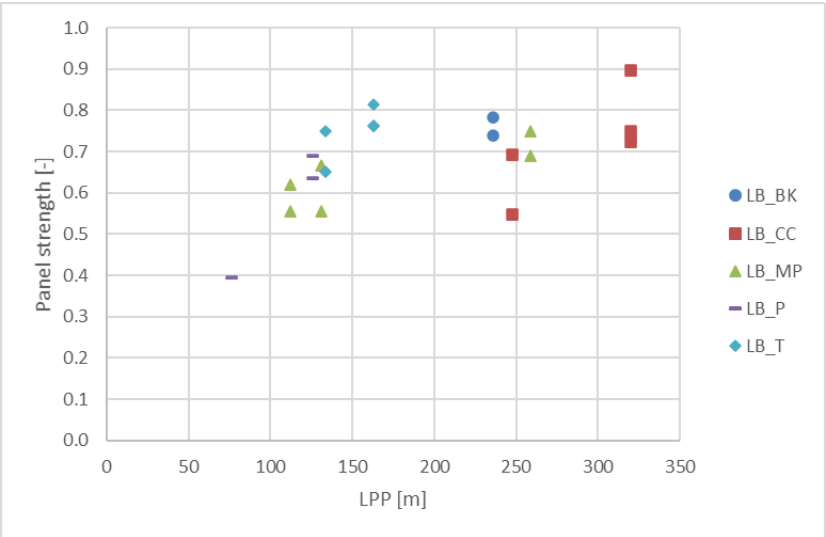

Figure 4.4. Longitudinal bulkhead panel compressive strength as a function of LPP [m]

A pattern is evident: independently of the considered ship type, longitudinal bulkhead panel strength increases with the increase in LPP values. This goes along with the overall trend regarding the increase

in panel strength with the increase in LPP, even though the plateau observed in the previously studied types of panels isn't so evident for longitudinal bulkhead panels.

The influence of LPP on longitudinal bulkhead panel strength is depicted in Figure 4.5.

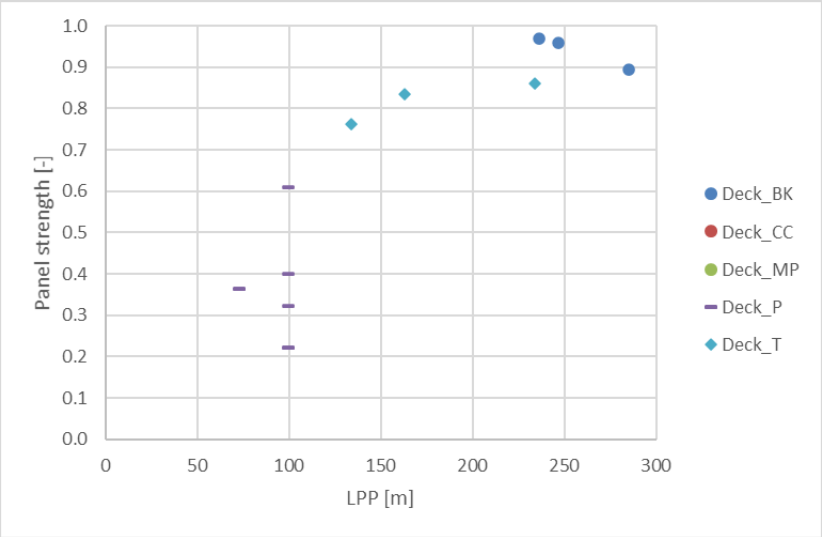

Figure 4.5. Deck panel compressive strength as a function of LPP [m]

Figure 4.5 displays that deck panels also follow the overall trend of increasing panel strength with increasing LPP values. The behaviour evidenced by deck panels regarding their strength, shows much higher values for cargo vessels (namely bulk carriers and tankers) when in comparison to passenger vessels. This is easily explained by the totally different magnitudes of loads which are expected to be considered for the design of say a tanker (with the amount of heavy machinery and structural reinforcements required for class and flag compliances) when compared to a passenger vessel, that is expected to withstand not much more than the passengers weight.

It must be pointed out that no deck panels from container carriers or multipurpose vessels were considered for this study, as ships of these types gathered in the database either didn't present decks in their structural arrangement or didn't present the adequate information for the purpose.

4.1.2. Influence of panel aspect ratio in panel strength

In this section, it is analysed and discussed the dependence of the compressive strength from the panel aspect ratio, α (defined in Equation [47]), for different locations: bottom, double bottom, side shell, longitudinal bulkhead and deck panels.

$$\alpha = \frac{l}{w_p} \quad [47]$$

It is presented the influence of local ship parameters on the panel strength in different ship panels. Besides, it is assessed if there is any pattern regarding both ship type and panel type.

The strength results regarding bottom panels presented in Figure 4.6 show how the evaluation of this variable as a function of panel aspect ratio leads to a cluster-like distribution.

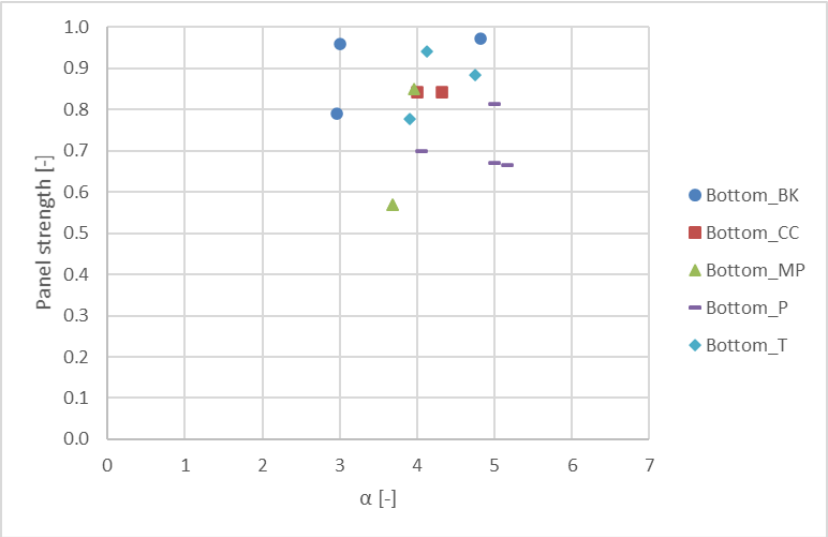

Figure 4.6. Bottom panel compressive strength as a function of panel aspect ratio, α

Most panel strength values seem to be dispersed around a central value of 0.8, with α values ranging from 3 to 5 (showing how the dispersion of this parameter is also very small).

Despite the concentration of bottom panel strength results, specific trends regarding each ship type can be found inside the cluster. Ship types such as bulk carriers and tanker vessels appear associated with the highest panel strength values from the cluster, with bulk carriers presenting a broader range of α values, while tanker bottom panels look more concentrated around an α of 4. On the other hand, multipurpose and passenger vessels are associated with the lowest portion of the cluster, translating how these ship types are associated with lowest panel strengths among bottom panels.

Next, the influence of α on the panel strength of double bottom panels was assessed, as shown in Figure 4.7.

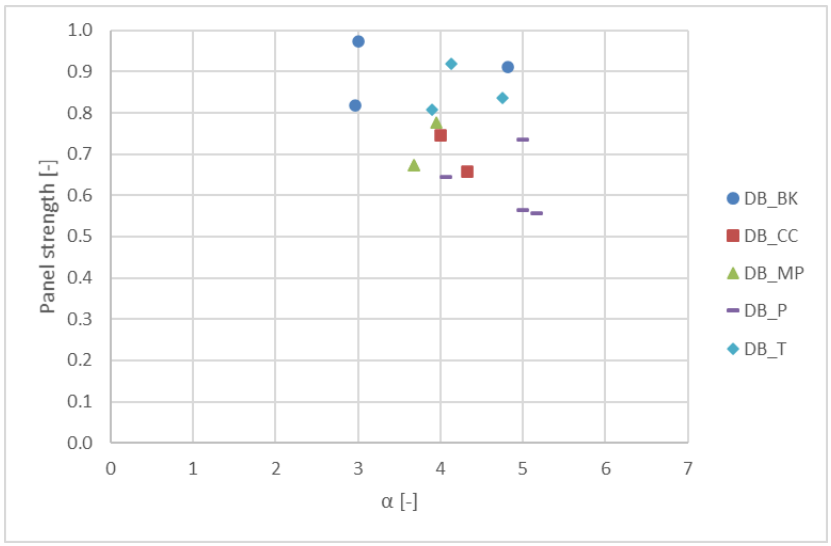

Figure 4.7. Double bottom panel compressive strength as a function of panel aspect ratio, α

When assessing the results obtained for double bottom panel strength as function of α, Figure 4.7 depicts a very similar behaviour in comparison with the results previously discussed for bottom panels. Once again, bulk carriers are associated with the highest strength values, and passenger vessels with the lowest panel strength values.

Although the strength values for double bottom panels present a concentration around 0.8, there's slightly more dispersion when comparing to the results obtained for bottom panels, with passenger vessels contributing to this effect with lower strength values at higher α values.

The results regarding side shell panel strength as function of panels aspect ratio are presented in Figure 4.8.

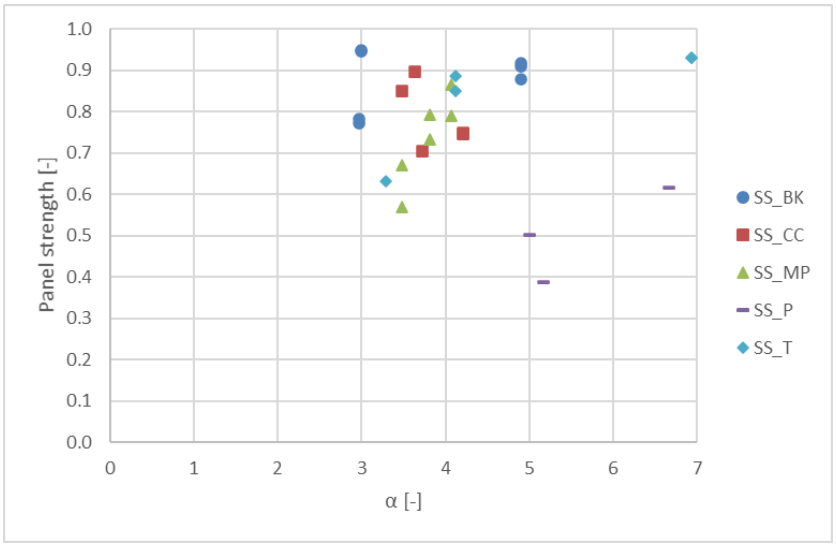

Figure 4.8. Side shell panel compressive strength as a function of panel aspect ratio, α

Figure 4.8 depicts further dispersion in comparison with both bottom and double bottom panel strength results as function of α. The side shell results present once again higher values associated with ship types such as bulk carriers and tankers, and the lowest values of panel strength associated with passenger vessels. In addition, these lower values of panel strength associated with passenger vessels (which present values around 0.5 with α higher than 5) deviate from the central data cluster, formed around the value of 0.8 with α values ranging from 3 to 5.

Regarding each ship type, a general trend in terms of α influence on side shell panel strength can be identified: except for container carriers, every other ship type presents an increase in panel strength with increasing α values, with multipurpose vessels presenting the highest gradient in its increase.

Afterwards, the longitudinal bulkhead results as a function of α are shown in Figure 4.9.

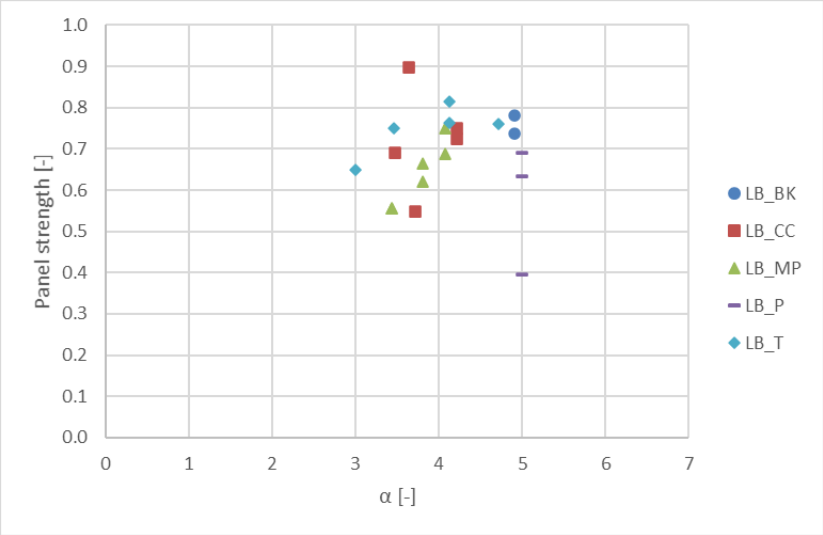

Figure 4.9. Longitudinal bulkhead panel compressive strength as a function of panel aspect ratio, α

The longitudinal bulkhead panel strength results presented in Figure 4.9 perfectly translate the cluster-like behaviour that has been mentioned throughout the several panel type studies regarding the influence of α in panel strength. Due to the little to no dispersion of the obtained results for longitudinal bulkhead panels, no specific patterns can be identified regarding each of the studied ship types.

Finally, the deck panel strength results with respect to α are depicted in Figure 4.10.

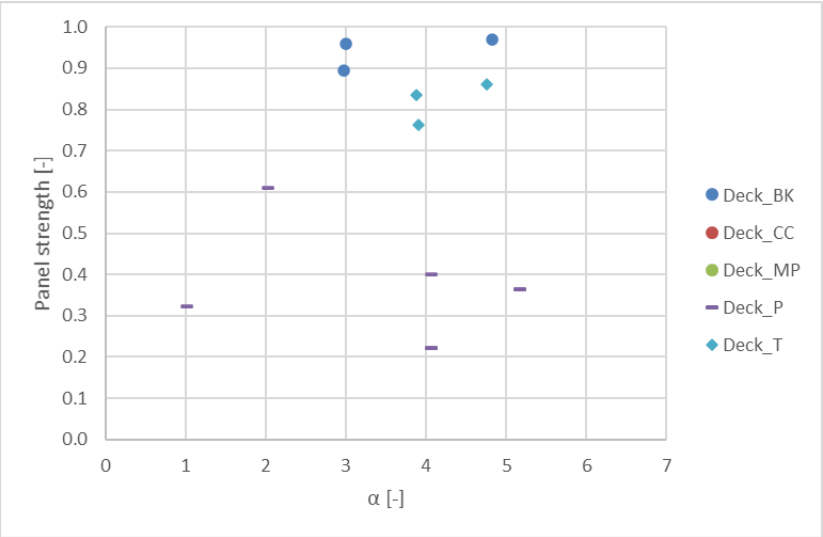

Figure 4.10. Deck panel compressive strength as a function of panel aspect ratio, α

The results for deck panel strength in Figure 4.10 translate the specificity of deck panels in comparison with other panel types. Not only certain ship types are not presented in this study (whether due to the absence of a deck structure in the structural arrangement or the lack of adequate information), but also the significant difference in terms of deck panel strength between cargo carrying vessels (in this case, bulk carriers and tankers) and passenger vessels, which is once again explained by the different load magnitudes which each of these ship types have to bear. In this case, the relation between deck panel compressive strength and panel aspect ratio doesn't present any relevant pattern.

4.1.3. Influence of corrosion additions on the stiffened panel strength results

In this chapter, the corrosion additions defined in Chapter 3.4.1 will be deducted from the original thicknesses, in order to assess how the eventual degradation of the structure (in this case, due to the expected corrosion) will affect the stiffened panel strength.

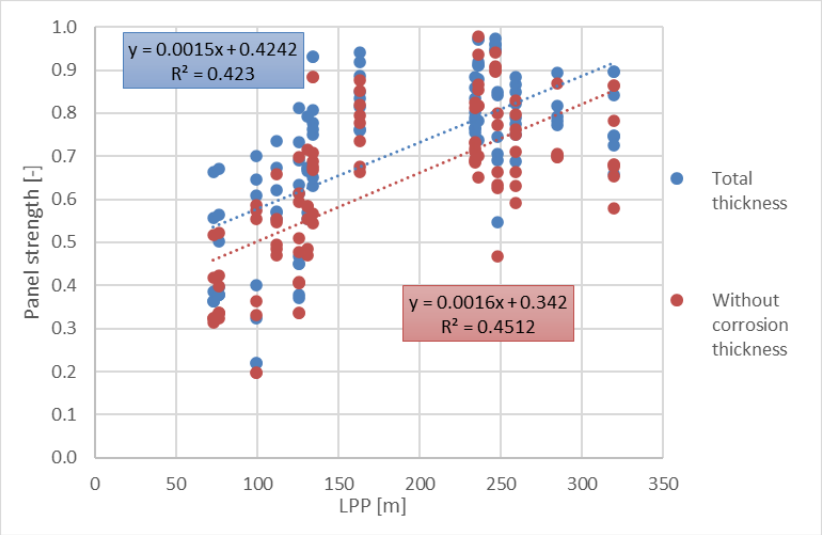

Figure 4.11. Overall influence of corrosion additions on stiffened panel strength

The results presented in Figure 4.11 show the stiffened panel strength results with and without the corrosion addition thicknesses, considering the entire panel scope. Overall, the decrease in panel strength is evident when deducting the corrosion additions and can be assessed by the corresponding fitting lines. This behaviour is expected, due to the significant decrease in structural material caused by the decrease in thickness.

However, the maximum value of panel strength obtained was associated with a panel where the corrosion addition was deducted. This fact can be explained by the different possible combinations between t_{c1} and t_{c2} and how that affects not only the column slenderness, but also the ratio between stiffener area and plate area (both defining variables for the stiffened panel strength).

4.2. Local strength assessment of secondary structure results

Accordingly with what had been determined in Chapter 3.5, the results of the local strength assessment of secondary structure will be presented in two distinct variations of the maximum bending stress expression shown in Equation [26]. The first one, shown in Equation [27], presents the ratio between maximum bending stress and lateral pressure, leading to the evaluation of the magnitude of the attained maximum bending stress for a given lateral pressure. The second one, shown in Equation [28], presents the lateral pressure value at which the attained maximum bending stress equals the yield stress.

Both variations will be analysed in two separate sections, the first to evaluate the influence of a ship-level variable (LPP), and the second one to evaluate the influence of a panel-level variable (α).

4.2.1. Influence of ship length on the local strength assessment

The ratio between maximum bending stress and lateral pressure was the first aspect analysed regarding the influence of ship length on the local strength assessment of secondary structure. First, it was assessed how LPP influenced the maximum bending stress over lateral pressure ratio for bottom panels.

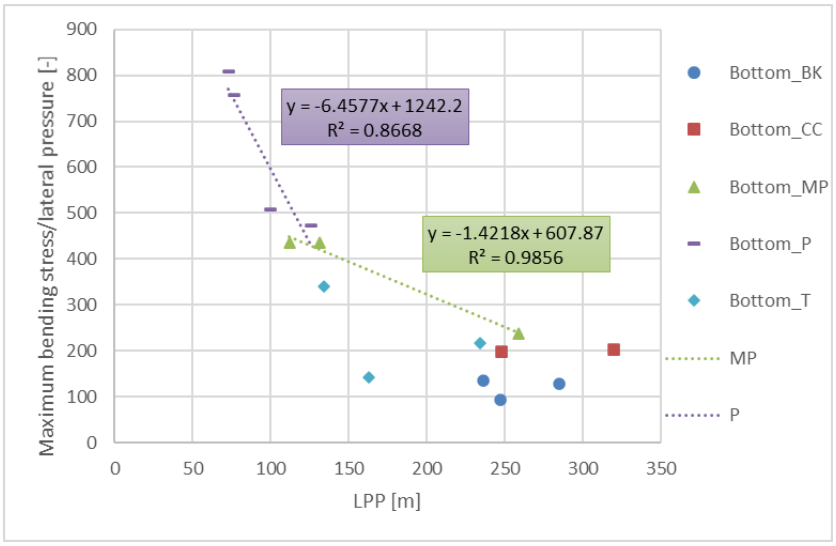

Figure 4.12. Maximum bending stress over lateral pressure for bottom panels as a function of LPP [m]

The maximum bending stress assessment results presented in Figure 4.12 for bottom panels show a general pattern of decrease with the increase in LPP. For smaller LPP values, the decrease in maximum bending stress is more significant when compared to vessels with higher LPP values. This can be assessed when comparing the results for passenger and multipurpose vessels, which have their fitting lines presented and the corresponding expressions highlighted in Figure 4.12. Equations [48] and [49] depict the fitting line expressions for passenger vessels and multipurpose vessels, respectively.

$$\frac{Maximum\ bending\ stress}{Lateral\ \ pressure} = -6.46 \times LPP + 1242 \qquad [48]$$

$$\frac{Maximum\ bending\ stress}{Lateral\ \ pressure} = -1.42 \times LPP + 608 \qquad [49]$$

Overall, one can conclude that vessels with higher LPP values present lower bending stresses for the same considered local lateral pressure, meaning that larger vessels are more suited to withstand local pressure loads with no structural compromise.

The maximum bending stress over lateral pressure ratio results as a function of LPP for double bottom panels are presented in Figure 4.13.

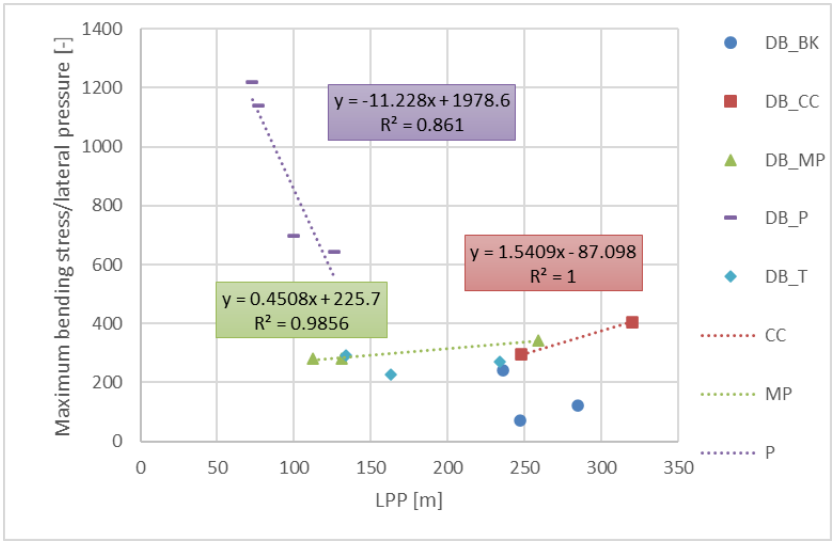

Figure 4.13. Maximum bending stress over lateral pressure for double bottom panels as a function of LPP [m]

Once again, for double bottom panels, the results shown in Figure 4.13 translate a decrease in maximum bending stress with increasingly higher LPP values. However, it must be pointed out how for these larger LPP values, the maximum bending stress tends to stabilize around a plateau. Some local increase tendencies can even be found for specific ship types, namely multipurpose (fitting line expression presented in Equation [50]) and container carrier vessels.

$$\frac{Maximum\ bending\ stress}{Lateral\ pressure} = 0.451 \times LPP + 226 \qquad [50]$$

The distinct change in the overall tendency that is verified for LPP values higher than 150 m, relates to the previously mentioned difference between the structural approach at a global (stiffened panel strength) and local (local strength assessment) level. For smaller sized vessels, the local approach will become more significant, while for larger vessels, the global approach considering longitudinal bending will be driving the design process. In this case, the increase in LPP won't translate into further decrease in the maximum bending stress, as vessels with these LPP values will only be affected at a global panel strength level.

Afterwards, it was assessed how LPP affected the maximum bending stress over lateral pressure ratio for side shell panels. The results are shown in Figure 4.14.

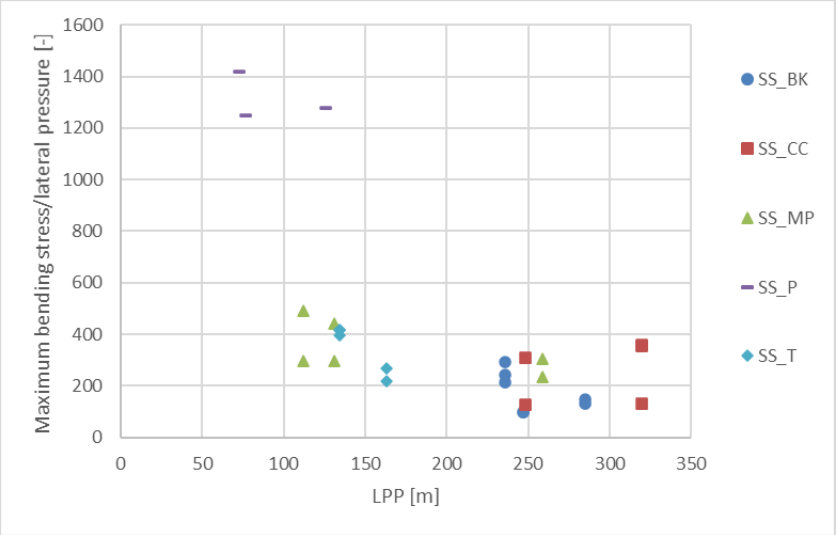

Figure 4.14. Maximum bending stress over lateral pressure for side shell panels as a function of LPP [m]

The results for the local strength assessment of side shell panels presented in Figure 4.14 doesn't present any significant differences with respect to the previously analysed panel types. Accordingly, side shell panels also present a steep decrease in maximum bending stress with the increase in LPP for LPP values up to 150 m. From this point on, and with further increase in LPP, the maximum bending stress tends to stabilize around an asymptotic value. Again, this behaviour is explained by the difference between the local and the global approaches dealt with in this study, and the way how they respectively influence smaller and larger vessels.

The results obtained for the local strength assessment of longitudinal bulkhead panels are presented in Figure 4.15.

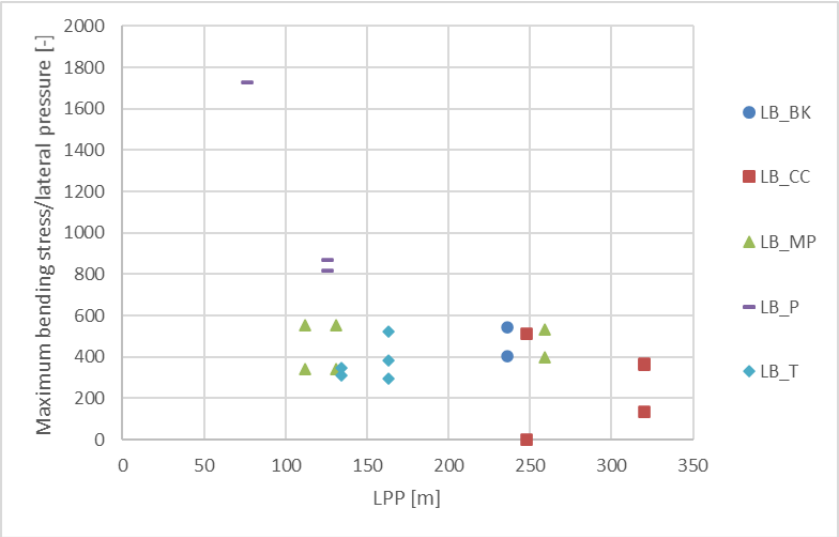

Figure 4.15. Maximum bending stress over lateral pressure for longitudinal bulkhead panels as a function of LPP [m]

Once again, and following the pattern previously observed for other panel types, the maximum bending stress shows a decrease with increasing LPP values, displaying a stabilization around a plateau, for LPP values higher than 150 m.

Finally, Figure 4.16 displays the results for the local strength assessment of deck panels.

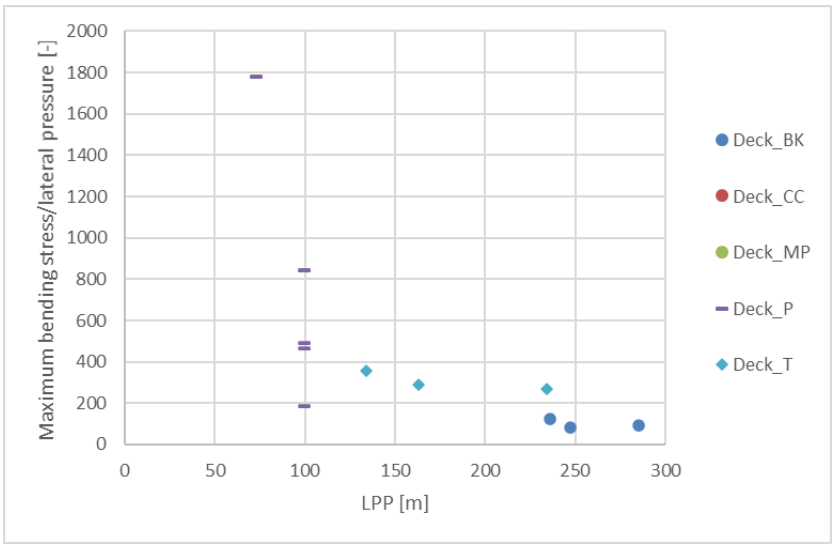

Figure 4.16. Maximum bending stress over lateral pressure for deck panels as a function of LPP [m]

Similarly to what was observed for the remaining panel types, an general decrease in maximum bending stress is evident when the considered LPP values increase. Besides, the same stabilization around an asymptotic value of maximum bending stress is also observed for higher LPP values (namely for LPP values over 150 m).

Afterwards, it was assessed how the ship's length affects the local lateral pressure to reach bending yield stress. The results presented in Figure 4.17 depict the influence of LPP on the pressure to reach bending yield stress for bottom panels.

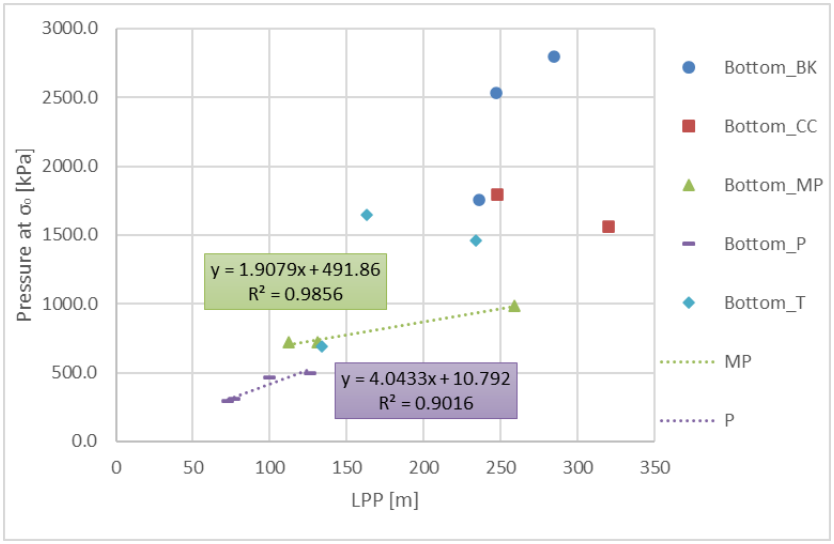

Figure 4.17. Pressure to reach bending yield stress for bottom panels as a function of LPP [m]

Considering the relation between the maximum bending stress over lateral pressure and the pressure to reach bending yield stress described in Chapter 3.5.1, the results are as expected. A visible increase in the pressure to reach bending yield stress with the increase in LPP, translates how larger vessels can withstand higher local lateral pressures to reach the respective bending yield stress, in comparison with smaller vessels.

Despite the overall linear behaviour, some visible linear tendencies within each ship type. This is observed for multipurpose and passenger vessels, which present high R^2 values with respect to the considered fitting lines (Equations [51] and [52], respectively). Besides, a significant dispersion is found for higher LPP values.

$$Pressure\ at\ \sigma_0 = 1.91 \times LPP + 492 \quad [51]$$

$$Pressure\ at\ \sigma_0 = 4.04 \times LPP + 10.8 \quad [52]$$

Figure 4.18 presents the pressure to reach bending yield stress results for double bottom panels.

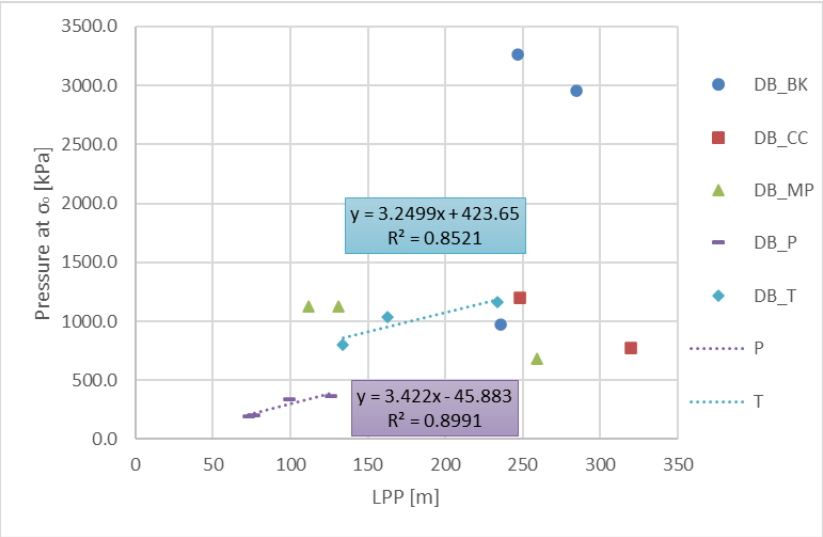

Figure 4.18. Pressure to reach bending yield stress for double bottom panels as a function of LPP [m]

Again, a general tendency of linear increase in pressure to reach bending yield stress with the increase in LPP is observed as expected. However, and similarly to what was observed for bottom panels in Figure 4.17, dispersion is observed when considering higher LPP values.

Linear trends for each considered ship type are also evident, namely considering passenger and tanker vessels. The respective fitting line expressions are shown in Equations [53] and [54]. The presented fitting lines for these ship types present high R^2 values, translating an appropriate relation, with neglectable dispersion.

$$Pressure\ at\ \sigma_0 = 3.42 \times LPP - 45.9 \quad [53]$$

$$Pressure\ at\ \sigma_0 = 3.25 \times LPP + 424 \quad [54]$$

The results for side shell panels shown in Figure 4.19 present some differences in comparison to what had been observed so far for both bottom and double bottom panels.

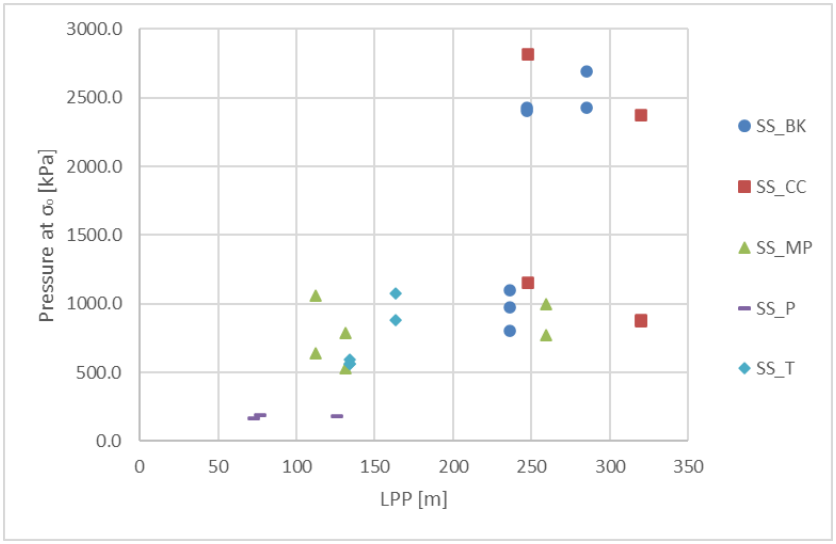

Figure 4.19. Pressure to reach bending yield stress for side shell panels as a function of LPP [m]

The overall linear increase of pressure to reach bending yield stress with increasing LPP values is still observed, however, the linear behaviour seems to present a smaller slope, restricted to smaller pressure values.

For larger LPP values, the pressure to reach bending yield stress isn't as high as, for instance, for double bottom panels. This fact is related to how for larger vessels the stiffened panel strength becomes the defining variable for the structural design. Therefore, and due to the smaller distance to the midship section neutral axis of side shell panels, these panels will require lower panel strength, and correspondingly, smaller pressures to reach bending yield stress.

The results regarding pressure to reach bending yield stress evidenced in Figure 4.20 translate the similarity between side shell and longitudinal bulkhead panels.

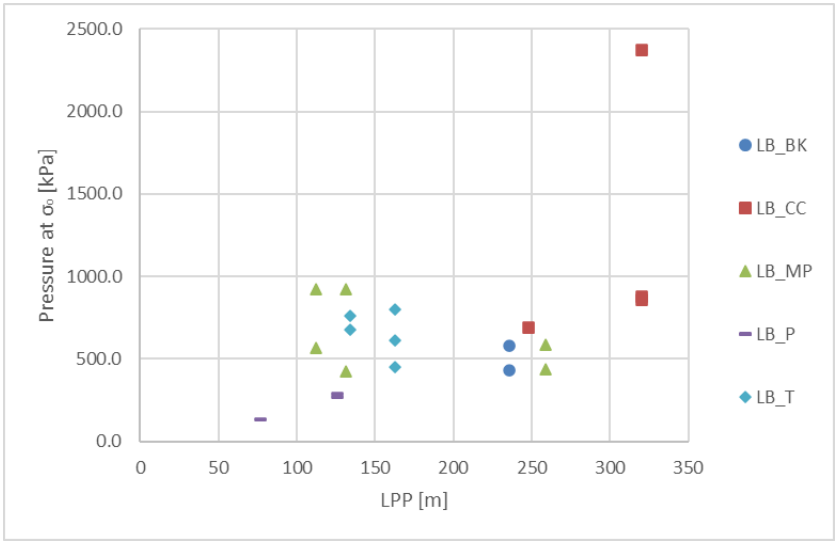

Figure 4.20. Pressure to reach bending yield stress for longitudinal bulkhead panels as a function of LPP [m]

The linear increase in pressure with the increase in LPP is once again verified, but with a smaller gradient in comparison with what was observed for bottom or double bottom panels. The resemblance regarding the results for side shell and longitudinal bulkhead panels is due to their similar location in the midship section, with lower distances to the neutral axis location.

Finally, it was assessed how the pressure to reach bending yield stress is affected by LPP in deck panels. The results are shown in Figure 4.21.

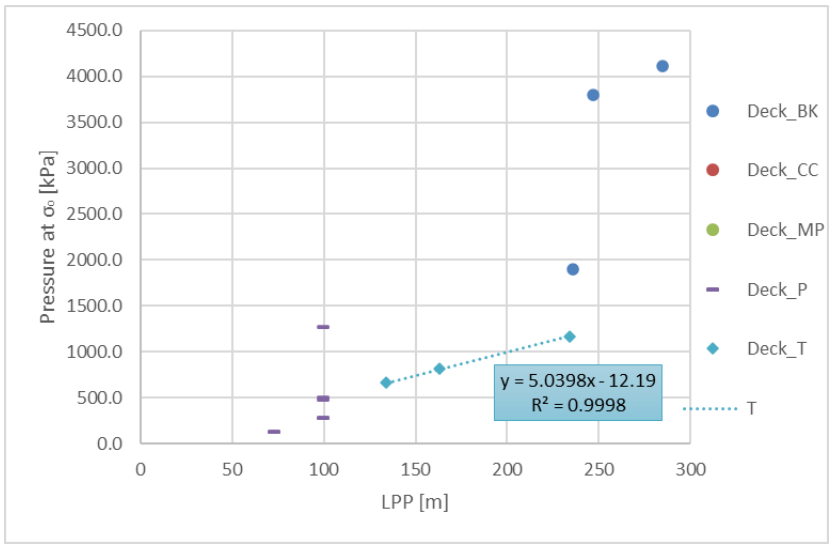

Figure 4.21. Pressure to reach bending yield stress for deck panels as a function of LPP [m]

The results shown in Figure 4.21 depict how the pressure to reach bending yield stress is influenced by LPP. Once more, the overall tendency of linear increase with increase in LPP is assessed, as it can be

drawn from the expression for the fitting line for the results regarding tanker vessels, presented in Equation [55].

$$Pressure\ at\ \sigma_0 = 5.04 \times LPP - 12.2 \quad [55]$$

Besides, the results gathered show significantly higher pressure values for the highest range of LPP (in this case associated with bulk carrier vessels). This can be due to the deck panels for these vessels being located at a significantly larger distance from the neutral axis than the remaining deck panel. Such evidence depicts, once again, how the stiffened panel strength becomes the driving variable for the structural design of larger vessels.

4.2.2. Influence of panel aspect ratio on the local strength assessment

Firstly, the influence of panel aspect ratio on the maximum bending stress over lateral pressure ratio will be assessed for several types of panels. Bottom panels will be addressed first, in Figure 4.22.

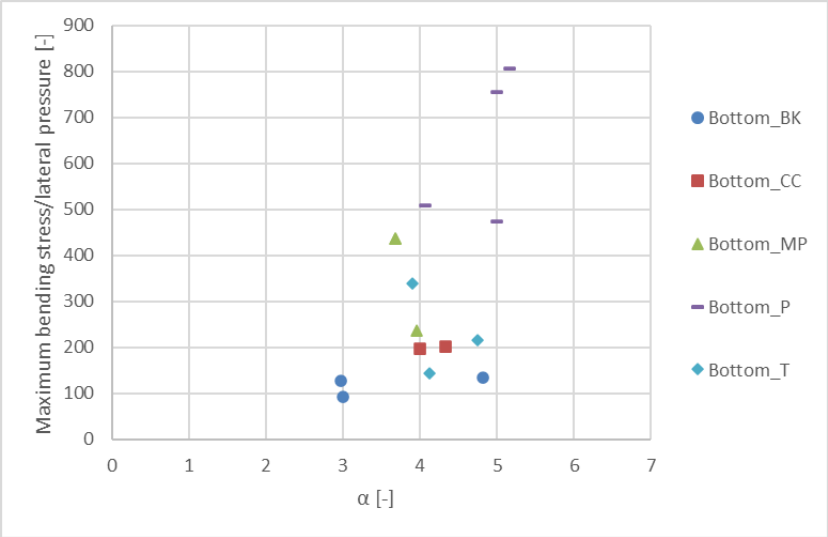

Figure 4.22. Maximum bending stress over lateral pressure for bottom panels as a function of panel aspect ratio, α

The results presented in Figure 4.22 translate an overall tendency of increase in maximum bending stress over lateral pressure with an increase in α. From the observed behaviour, one can argue that stockier panels (presenting lower α values) are better prepared to withstand higher lateral pressures. In the case of bottom panels, cargo carrying vessels (bulk carriers, container carriers, tankers and multipurpose vessels) appear associated with the lower values of maximum bending stress, while passenger vessels present correspondingly higher maximum bending stresses and α values.

The expression derived for the maximum bending stress over lateral pressure (defined in Equation [27]) also gives an indication of this fact. The l^2 term present on the numerator of Equation [27] indicates a squared increase in maximum bending stress over lateral pressure with the increase in frame spacing, which itself leads to the increase of the panel aspect ratio, α.

Figure 4.23 depicts the results of maximum bending stress over lateral pressure as a function of α for double bottom panels.

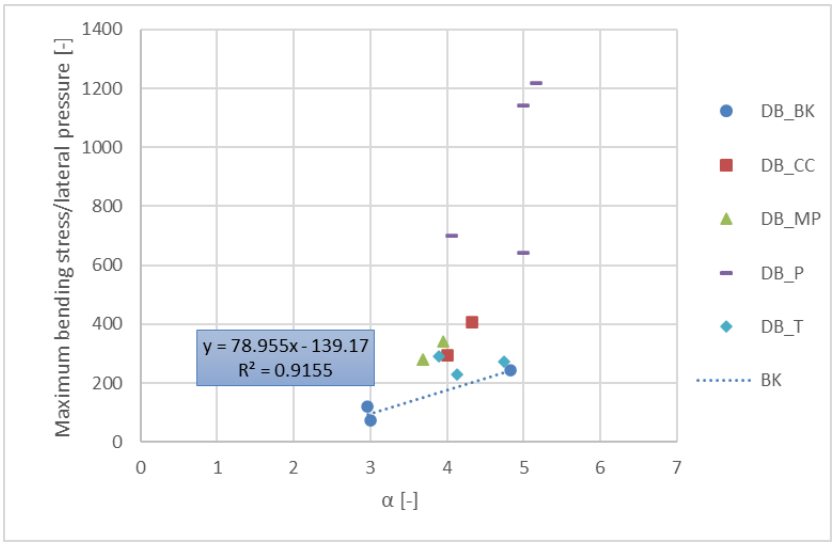

Figure 4.23. Maximum bending stress over lateral pressure for double bottom panels as a function of panel aspect ratio, α

Similarly to what was observed in Figure 4.22 for bottom panels, a general linear increase in maximum bending stress over lateral pressure is verified with the increase in α.

Once again, the panels corresponding to cargo vessels appear associated with the lower maximum bending stresses. This can be assessed namely considering bulk carrier vessels, which present an evident linear behaviour, as it can be assessed through its fitting line expression shown in Equation [56]. These lower maximum bending stress values are associated with cases where the panel is dimensioned to withstand higher lateral pressures without generating high stresses.

$$\frac{Maximum\ bending\ stress}{Lateral\ pressure} = 79.0 \times \alpha - 139 \qquad [56]$$

The side shell panel results for maximum bending stress over lateral pressure as function of α shown in Figure 4.24 present linear trends within specific ship types.

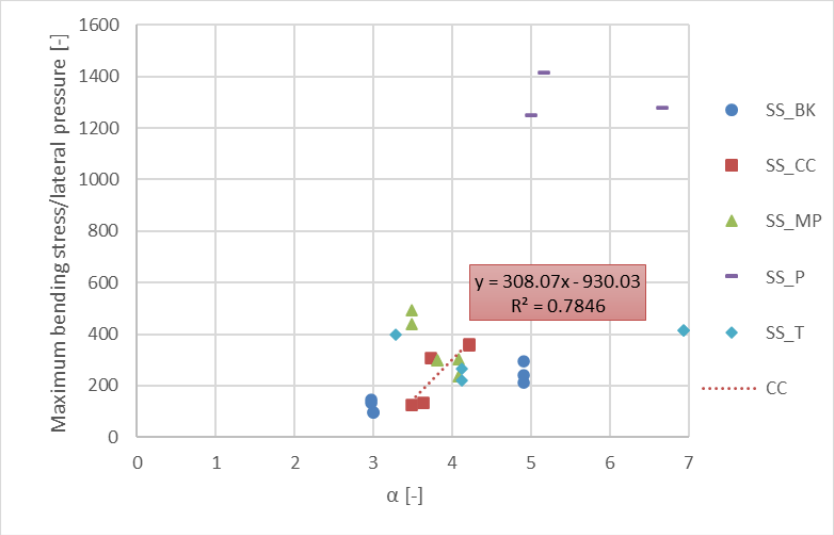

Figure 4.24. Maximum bending stress over lateral pressure for side shell panels as a function of panel aspect ratio, α

A good example of this can be found for container carrier vessels, which present a linear relation between the maximum bending stress and panel aspect ratio, as shown in Equation [57], the corresponding fitting line expression.

$$\frac{Maximum\ bending\ stress}{Lateral\ pressure} = 308 \times \alpha - 930 \qquad [57]$$

However, the overall behaviour for this panel type is of a cluster-like concentration around a maximum bending stress over lateral pressure ratio of 300. Moreover, the results for passenger vessels are found to be significantly dispersed from this mentioned cluster, associated with higher bending stress over pressure ratios and slenderer panels.

Figure 4.25 depicts the maximum bending stress over lateral pressure results as function of α for longitudinal bulkhead panels.

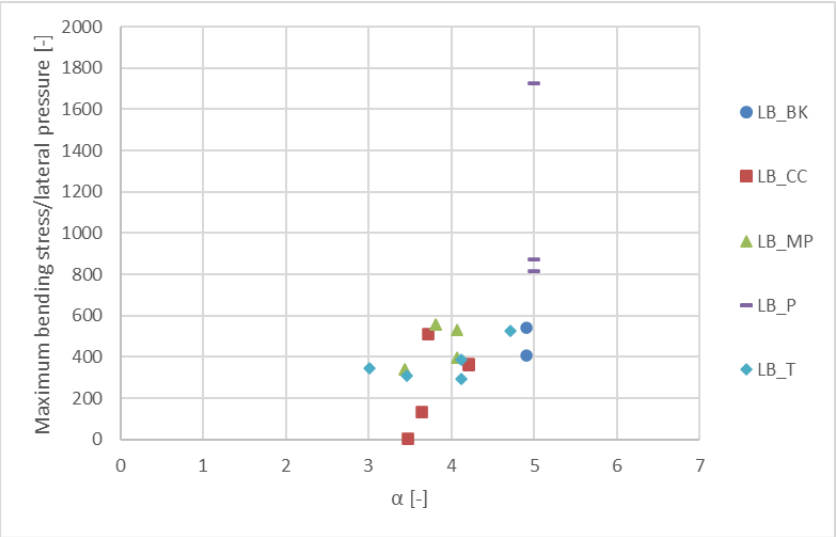

Figure 4.25. Maximum bending stress over lateral pressure for longitudinal bulkhead panels as a function of panel aspect ratio, α

A general tendency of increase in maximum bending stress over lateral pressure is observed when α increases, in agreement with had been observed in Figure 4.22 and Figure 4.23 for bottom and double bottom panels, respectively.

The results of maximum bending stress over lateral pressure as function of α for deck panels are displayed in Figure 4.26.

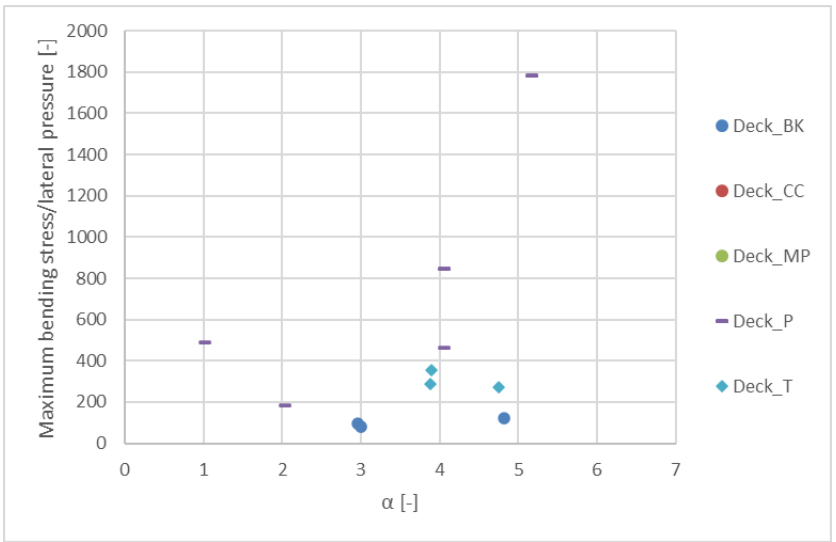

Figure 4.26. Maximum bending stress over lateral pressure for deck panels as a function of panel aspect ratio, α

No apparent relation is found between the considered variables. A similar situation had been observed on another study regarding deck panels, when assessing the influence of the variation of α on the deck panel compressive strength (Figure 4.10).

Secondly, the influence of panel aspect ratio on the pressure to reach bending yield stress was assessed for different panel types. The results regarding the influence of α on the pressure to reach bending yield stress for bottom panels are presented in Figure 4.27.

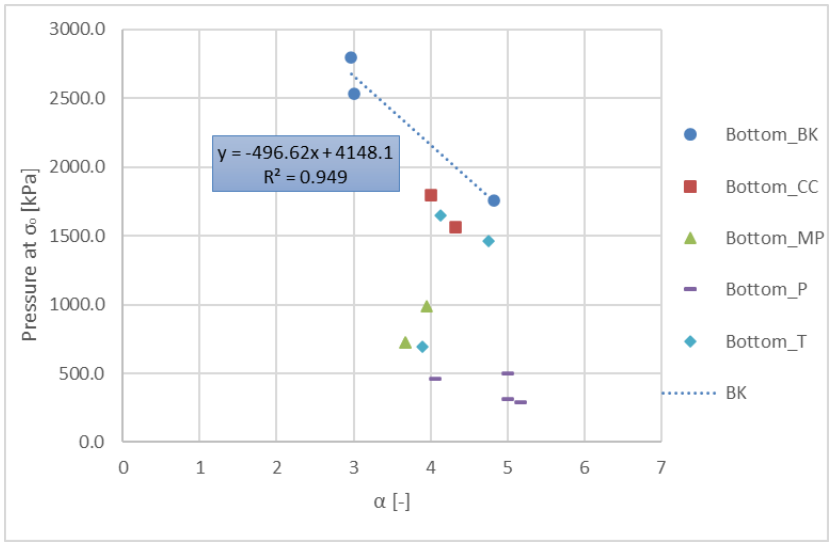

Figure 4.27. Pressure to reach bending yield stress for bottom panels as a function of panel aspect ratio, α

An overall tendency of decrease in the pressure to reach bending yield stress with increasingly higher α values is verified. However, one can clearly assess how the data regarding bulk carrier, container carrier and tanker vessels is associated with the top tier in terms of pressure values, while the results for multipurpose and passenger vessels appear associated with the set of lower pressure values.

Once again, the tendency previously observed when assessing the influence of the panel aspect ratio on the maximum bending stress over lateral pressure is verified. Stockier panels (with lower α values) require higher lateral pressures to reach the bending yield stress, hence being able to withstand higher pressures than slenderer panels, for the same stress level.

Figure 4.28 presents the results regarding the influence of panel aspect ratio on the pressure to reach bending yield stress.

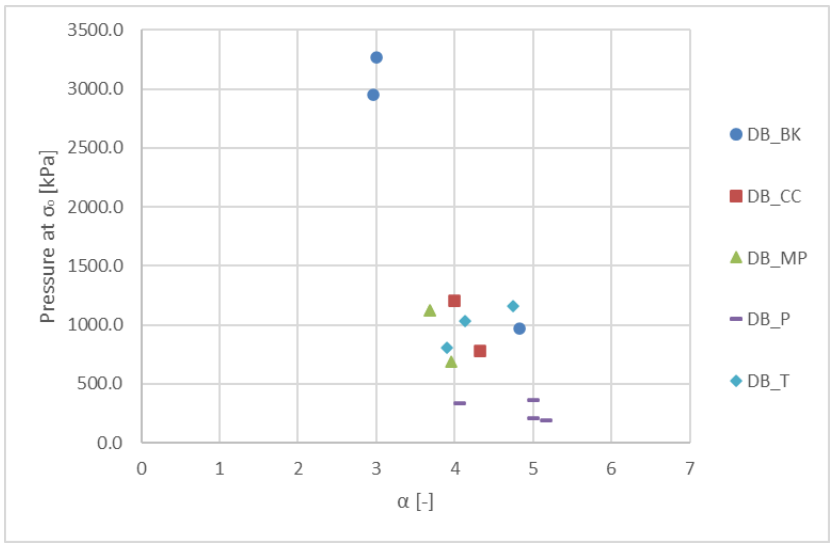

Figure 4.28. Pressure to reach bending yield stress for double bottom panels as a function of panel aspect ratio, α

Overall, it is observed a concentration of most of the results around a cluster located around a lateral pressure of 800 kPa. The concentration of values translates how the dimensioning of the considered double bottom panels tends to be similar, in spite of eventual differences in terms of ship type or even LPP.

The results shown in Figure 4.29 allow to assess the influence of the panel aspect ratio on the pressure to reach bending yield stress, for side shell panels.

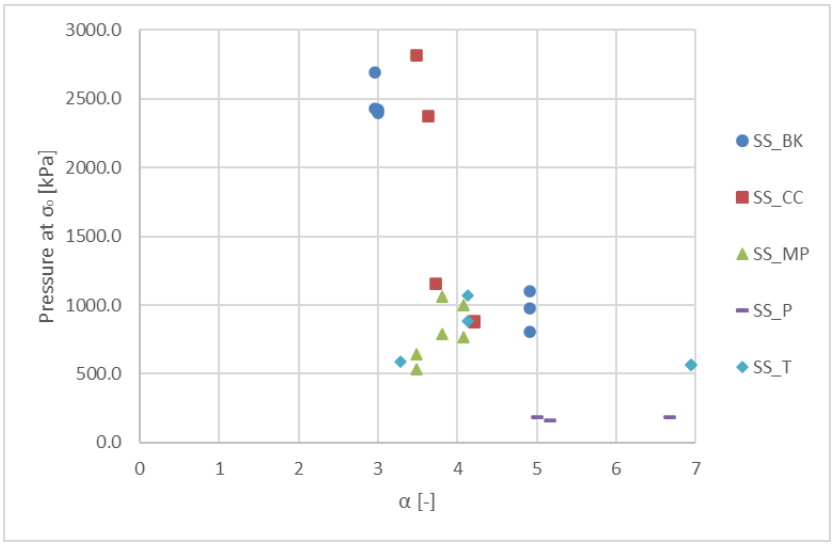

Figure 4.29. Pressure to reach bending yield stress for side shell panels as a function of panel aspect ratio, α

In this case, three distinct clusters can be identified: one around 2500 kPa for α values around 3, one around 1000 kPa for α values around 4 and one around 200 kPa for α values between 5 and 7. These

three consecutive clusters allow to assess a global tendency of decrease in pressure to reach bending yield stress with slenderer panels (larger α values).

It's also interesting to notice how different ship types are associated with each of the observed clusters. The first cluster (larger pressures and lower α values) is composed of bulk and container carriers, while the second (intermediate pressures and α values) consist of mostly multipurpose and tanker vessels, while the final cluster (lower pressures and higher α values) is composed of passenger vessels.

The longitudinal bulkhead panel results for pressure to reach bending yield stress as a function of α are depicted in Figure 4.30.

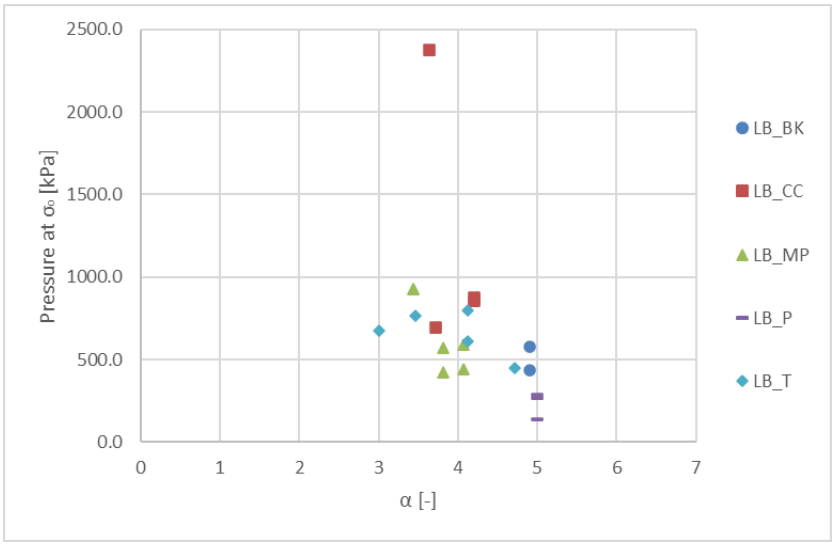

Figure 4.30. Pressure to reach bending yield stress for longitudinal bulkhead panels as a function of panel aspect ratio, α

An inversely proportional behaviour is observed, when assessing the influence of the panel aspect ratio on the pressure to reach bending yield stress.

Besides, it is visible how for longitudinal bulkhead panels, the pressures to reach bending yield stress are, in general, significantly lower than, for instance, for bottom panels (Figure 4.27). This difference can be due to the difference in the location of the mentioned panels in the midship section. Consequently, the distance between the panel and the corresponding midship section neutral axis becomes the defining variable for the dimensioning of the considered panels, due to the influence this aspect has on the loads the panel must endure. Since bottom panels are normally located farther form the neutral axis than longitudinal bulkhead panels, it's only natural that these panels are dimensioned to withstand larger lateral pressures than, in this case, longitudinal bulkhead panels.

The results for deck panels concerning the influence of α on the pressure to reach bending yield stress are presented in Figure 4.31.

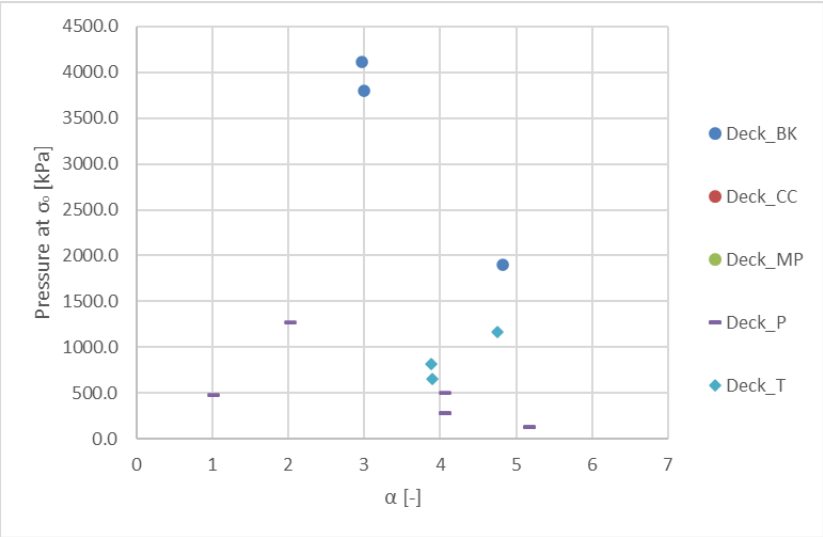

Figure 4.31. Pressure to reach bending yield stress for deck panels as a function of panel aspect ratio, α

Once again, and in line with what was observed in Figure 4.26 for the maximum bending yield stress over lateral pressure results, the results presented in Figure 4.31 show no relevant relation between the pressure to reach bending yield stress and α.

4.2.3. Influence of corrosion additions on the local strength assessment results

In this chapter, the influence of corrosion additions on the local strength assessment will be studied. Both the maximum bending stress over lateral pressure and the pressure to reach bending yield stress will be analysed as a function of LPP, when considering the thicknesses with deducted corrosion additions. Bottom panels were chosen for this study, due to the evident behaviour presented in Figure 4.12 and Figure 4.17.

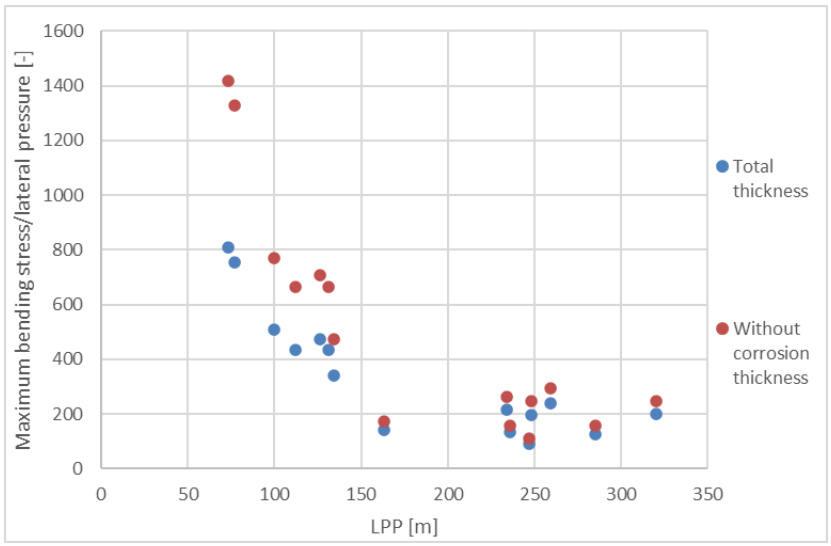

Figure 4.32. Influence of corrosion additions on maximum bending stress over lateral pressure for bottom panels

The results presented in Figure 4.32 translate an increase in maximum bending stress, when deducting the respective corrosion additions to the original plate and stiffener thicknesses. This behaviour is expected, as with the decrease in the amount of structural material, due to the thickness decrease, the structure will present higher stresses for the same load case.

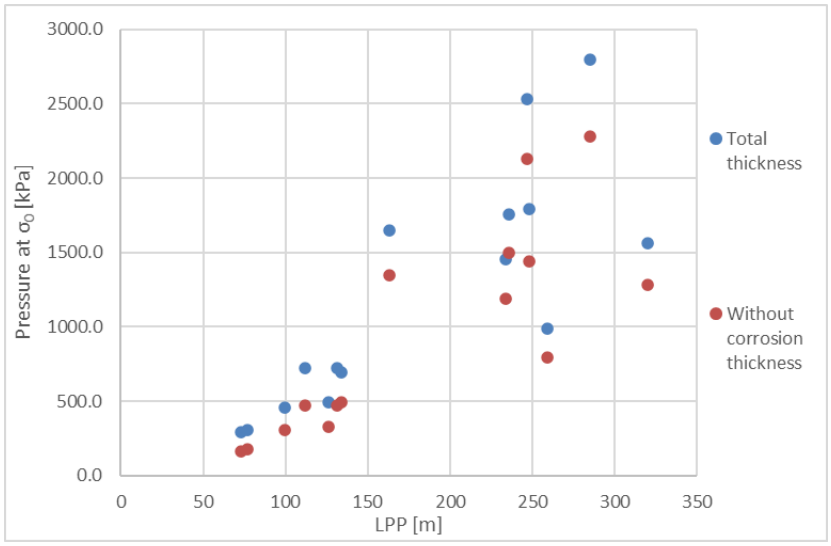

Figure 4.33. Influence of corrosion additions on pressure to reach bending yield stress for bottom panels

Figure 4.33 depicts the results for pressure to reach bending yield stress when considering the corrosion additions. Accordingly with what was observed in Figure 4.32, the values of the pressures to reach bending yield stress drop when considering the corrosion addition deductions on the original thicknesses of the panel. The decrease in the amount of structural material leads to reaching bending yield stress

with lower lateral pressures applied, making it easier for the panel to reach a higher bending stress state.

4.3. Production costs results

In the present chapter, the production costs introduced in Chapter 3.6 will be analysed in two distinct ways: production costs per unit area and production costs per unit weight. In the first one, the total production costs of each panel are divided by the panel's area, while on the second one the same production costs are divided by the panel's weight. Both studies will present production costs results as a function of LPP.

The main objective of this distinction is to assess how differently the two main characteristics of a shipbuilding panel – its area and weight – impact the overall production costs. This distinction is of particular interest when considering situations where a shipyard that is evaluating the feasibility of a certain type of panel must deal with restrictions. These can either relate to available workshop space (where area is the defining variable) or lifting capacity of the shipyard machinery (where weight is the defining variable).

Besides, a comparative study between the production costs of each panel type and the respective bottom panel production costs was carried out regarding both costs per unit area and weight. Using the ratio between the production cost of each considered panel and the production cost of the respective bottom panel, it becomes possible to evaluate trends with respect to a benchmark value of each of the ships in the database.

4.3.1. Overall production costs per unit area

In the present chapter, the results regarding the total panel production costs per unit area (TPPCA) are presented, and its dependence regarding corresponding LPP values is analysed. Initially, the TPPCA results are presented with no distinction in terms of either ship or panel type. Subsequently, the plots of TPPCA for each different ship type are shown, and within each ship type, tendencies regarding different panel types will be assessed.

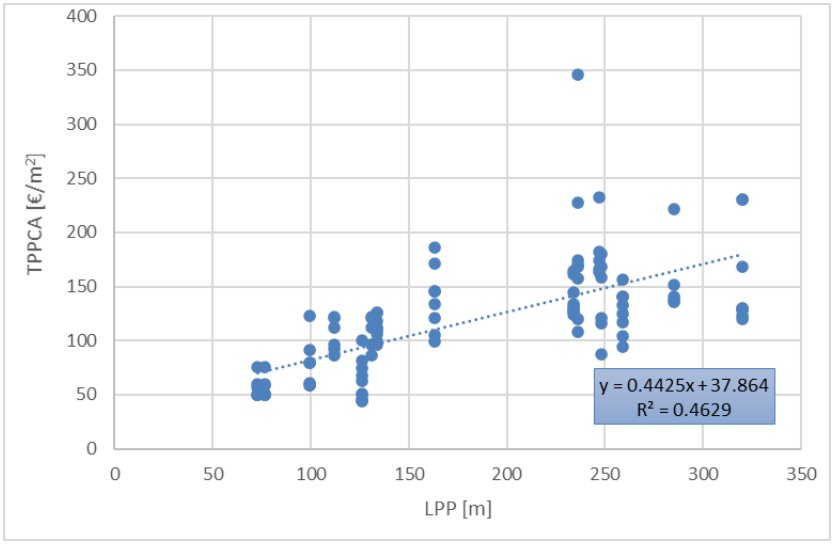

Figure 4.34. TPPCA [€/m^2] as a function of LPP [m]

In general, Figure 4.34 shows how TPPCA are directly proportional to the LPP of the considered ship, as seen in Equation [58], the fitting line expression.

$$TPPCA = 0.443 \times LPP + 37.9 \quad [58]$$

Two distinct behaviours can be observed, depending on the considered range of LPP. For LPP values lower than 200 m, a clear linear increase in TPPCA with increase in LPP is found. On the other hand, for LPP values higher than 200 m, the TPPCA seem to remain constant despite the increase in LPP (disregarding some of the observed dispersion). These distinct tendencies are related to the two different LPP ranges that define the ship types considered in the significant ship database. While the lowest LPP range is associated with passenger and multipurpose vessels, the highest LPP range is associated with tanker, bulk and container carrier vessels.

Nonetheless, with increasingly higher LPP values (namely in the LPP range of 250 to 325 m), the previously mentioned dispersion from the general linear behaviour becomes evident, with both higher and lower values of production costs. The dispersion from the general linear behaviour can be assessed from the low R^2 value presented with respect to the fitting line, which indicates significant dispersion from the fitting expression.

Figure 4.35 presents the results of TPPCA as a function of LPP for bulk carrier vessels.

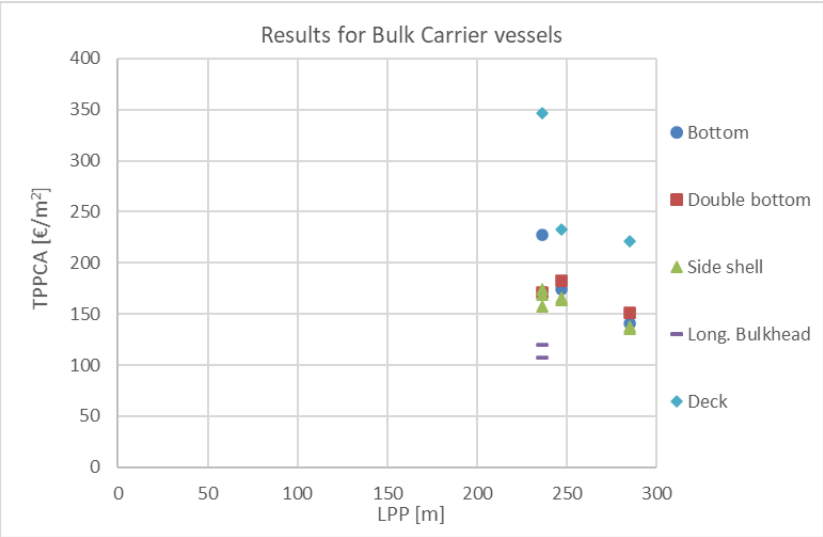

Figure 4.35. TPPCA [€/m^2] as a function of LPP [m] for bulk carrier vessels

Since bulk carrier vessels are associated with the highest LPP values, it becomes natural that the results presented in Figure 4.35 correspond to the highest values from the entire scope of the results shown in Figure 4.34.

An interesting fact that can be drawn from these results is how panel types such as bottom, double bottom and side shell present a decrease in production costs with an increase in LPP values. This evidences how, in specific situations, the increase in LPP, which is usually associated with higher bending moments to account for, doesn't necessarily mean an increase in structural reinforcement and therefore production costs.

The results of TPPCA as a function of LPP for container carrier vessels are depicted in Figure 4.36.

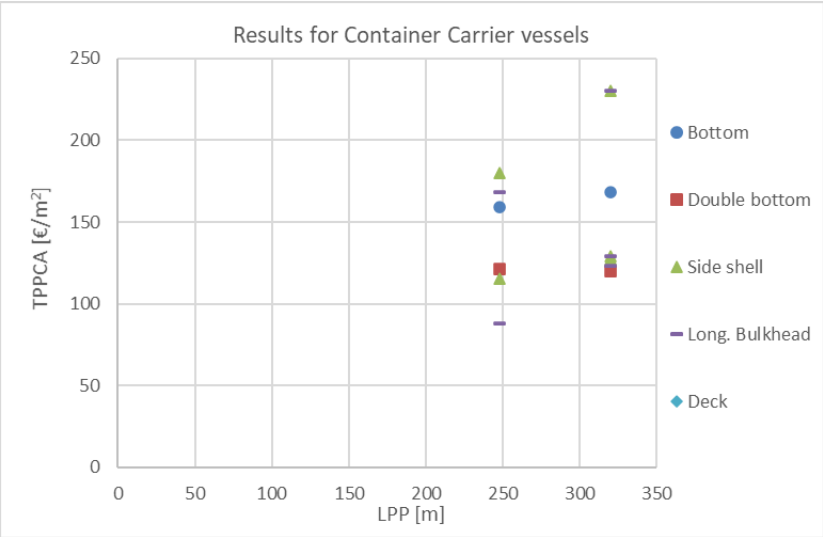

Figure 4.36. TPPCA [€/m^2] as a function of LPP [m] for container carrier vessels

Container carrier vessels are also associated with the highest range of LPP values in the database (250 to 325 m). Accordingly, the production cost results presented in Figure 4.36 translate the scattering of the TPPCA with LPP that is observed for much of the data. This mentioned dispersion leads to a difficulty when assessing patterns regarding each different panel type.

The short number of database entries regarding container carriers is also severely compromising a proper evaluation of any tendencies regarding this ship type, as only two LPP values can induce inadequate generalizations.

Figure 4.37 depicts how TPPCA are influenced by LPP for multipurpose vessels.

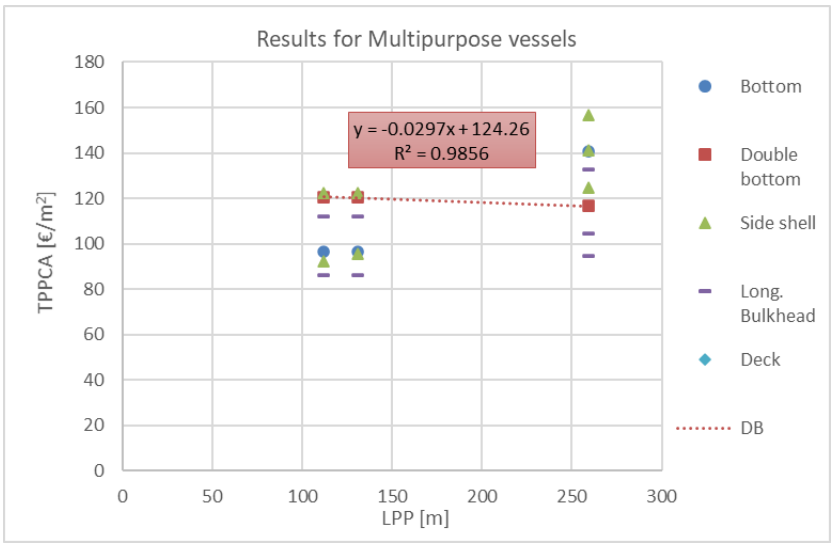

Figure 4.37. TPPCA [€/m^2] as a function of LPP [m] for multipurpose vessels

The results of TPPCA shown in Figure 4.37 for multipurpose vessels depict a clear linear pattern in the increase of the costs with the increase in LPP. The increase seems more evident regarding both longitudinal panel types (side shell and longitudinal bulkhead panels), however, with double bottom panels an almost constant behaviour is visible, with a slight tendency to decrease, as seen in the fitting line expression presented in Equation [59].

$$TPPCA = -0.0297 \times LPP + 124 \quad [59]$$

The results of TPPCA as a function of LPP for passenger vessels are depicted in Figure 4.38.

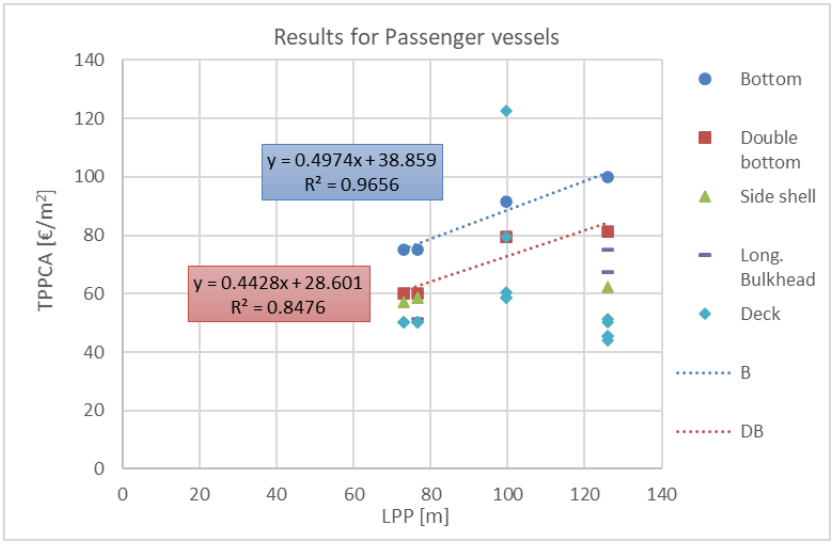

Figure 4.38. TPPCA [€/m^2] as a function of LPP [m] for passenger vessels

Passenger vessels present some different tendencies regarding each of the different considered types of panels. Figure 4.38 shows how for passenger vessels production costs increase with an increase in LPP, as visible in the fitting line expressions of both bottom (Equation [60]) and double bottom panel types (Equation [61]) and respective R^2 values. On the other hand, side shell panels seem to remain pretty much constant with different LPP values. Besides, the deck panel results translate no relation whatsoever, as there's serious dispersion regarding the TPPCA with respect to LPP.

$$TPPCA = 0.497 \times LPP + 38.9 \quad [60]$$

$$TPPCA = 0.443 \times LPP + 28.6 \quad [61]$$

At last, Figure 4.39 depicts how TPPCA are influenced by LPP for multipurpose vessels.

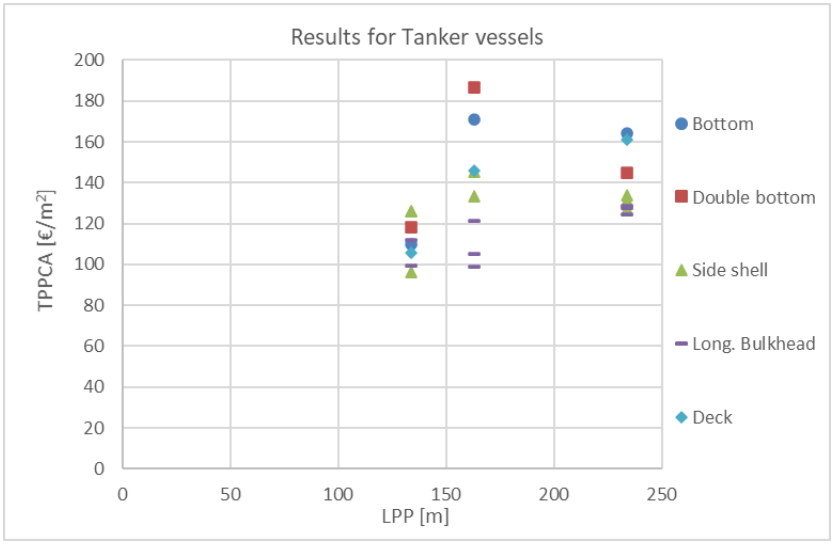

Figure 4.39. TPPCA [€/m^2] as a function of LPP [m] for tanker vessels

Figure 4.39 shows an overall tendency of linear increase of TPPCA with increase in LPP, with bottom, side shell, longitudinal bulkhead and deck panels depicting this mentioned behaviour. Some dispersion is verified around the LPP value of 160 m, leading to a local maximum for double bottom TPPCA.

Although no specific trend can be observed as common to every ship type or panel type, throughout the present chapter some relevant remarks have been made in terms of the relation between TPPCA and LPP. Ship types such as multipurpose and tanker vessels presented a linear increase in TPPCA with an increase in LPP across all the considered panel types. However, some of the considered panel types associated with bulk carriers, namely bottom, double bottom, and side shell panels, presented a decrease in TPPCA with an increase in LPP. Besides, several situations showed no relation whatsoever between the regarded panel production costs and LPP, for instance in the container carrier results presented in Figure 4.36.

4.3.2. Panel production costs per unit area: a comparative analysis regarding bottom panels production costs

In this section, the ratio between the TPPCA of each panel type and the TPPCA of the corresponding bottom panel is analysed as a function of LPP. The mentioned ratio is defined in Equation [62].

$$\frac{TPPCA_{chosen\ panel}^{ship\ n}}{TPPCA_{bottom\ panel}^{ship\ n}} \quad [62]$$

This assessment aims at understanding how larger or smaller the TPPCA of each panel type are in comparison to the TPPCA of bottom panels.

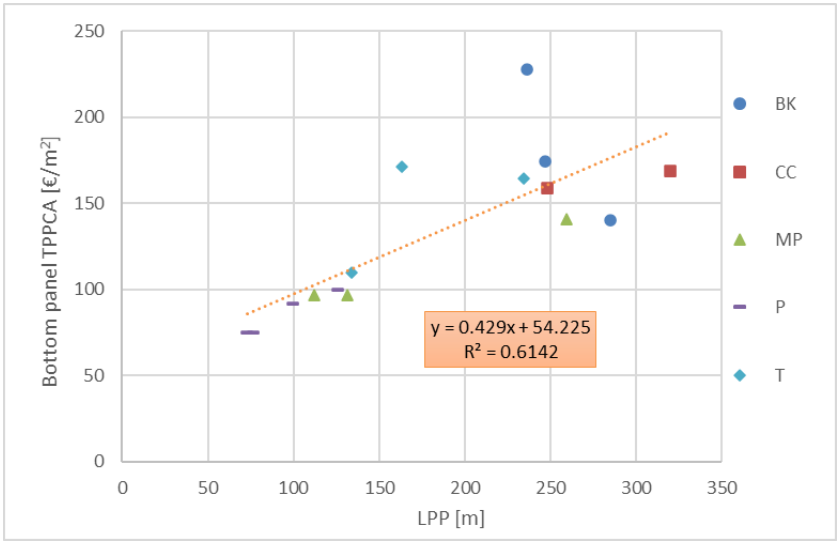

Figure 4.40. TPPCA [€/m^2] as a function of LPP [m] for bottom panels

The TPPCA results for bottom panels are shown in Figure 4.40, presenting a global linear increase in TPPCA with increasingly higher LPP values (evident when considering the presented overall fitting line expression, Equation [63]).

$$TPPCA = 0.429 \times LPP + 54.2 \qquad [63]$$

Bottom panels were defined as the benchmark for this comparison, as they are usually the stiffest panels of the midship section, usually presenting the highest amount of structural material and, as observed in Chapter 4.3.1, the highest TPPCA in general.

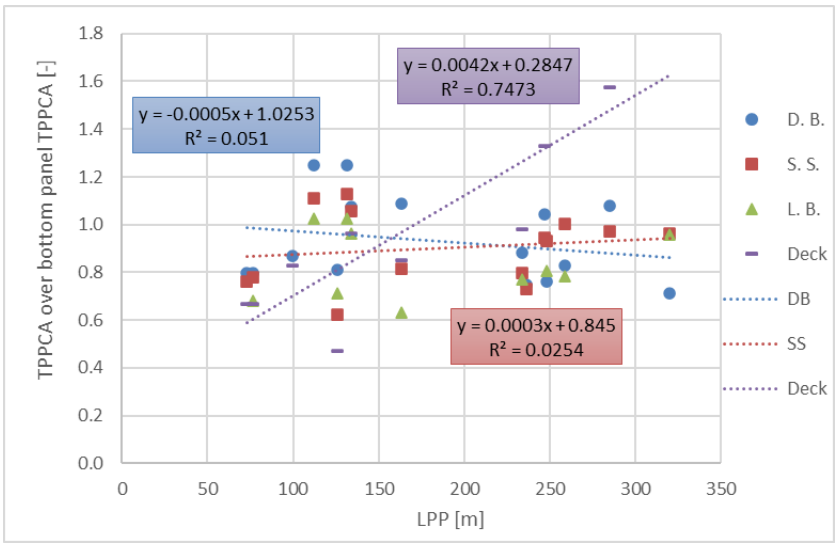

Figure 4.41. TPPCA over bottom TPPCA as a function of LPP [m]

The results presented in Figure 4.41 depict two distinct trends. For double bottom, side shell and longitudinal bulkhead panels, not only the ratio between each TPPCA and bottom TPPCA remains asymptotically constant throughout the entire LPP scope, but it remains constant around the value of 1 (this can be seen for example in the fitting line expressions presented in Equations [64] and [65]). On the other hand, for deck panels, the ratio between TPPCA and bottom TPPCA presents a linear behaviour, increasing with increasingly higher LPP values.

$$\frac{TPPCA_{double\ bottom}}{TPPCA_{bottom}} = -0.0005 \times LPP + 1.03 \quad [64]$$

$$\frac{TPPCA_{side\ shell}}{TPPCA_{bottom}} = 0.0003 \times LPP + 0.845 \quad [65]$$

The observed patterns allow to conclude that the TPPCA regarding double bottom, side shell and longitudinal bulkhead panels is dependent on the TPPCA of the considered vessel, not on the LPP. Nonetheless, and since the influence of LPP on the TPPCA of bottom panels has been assessed throughout Chapter 4.3.1, one can argue that the TPPCA of other panel types is indirectly dependent of the LPP. For deck panels, however, smaller vessels tend to present TPPCA lower than the corresponding bottom panel TPPCA, with larger vessels showing increasingly higher TPPCA with respect to the bottom panel TPPCA.

4.3.3. Overall production costs per unit weight

In this chapter, the results concerning the influence of LPP on the total panel production costs per unit weight (TPPCW) are presented. First, the results regarding TPPCW are presented with no distinction in terms of either ship or panel type. Secondly, the TPPCW results are presented for each type of ship. An analysis will be carried out in each case, not only to assess tendencies evident for each ship type, but also in terms of tendencies noticeable for different panel types within each ship type.

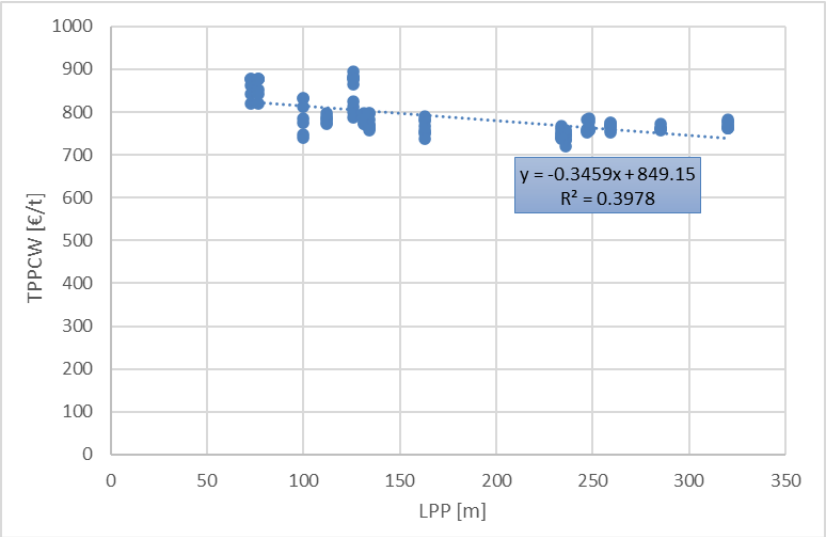

Figure 4.42. TPPCW [€/t] as a function of LPP [m]

Figure 4.42 presents the overall TPPCW results as a function of LPP. A slight decrease in the TPPCW is observed with increase in LPP, as assessed in the fitting line expression presented in Equation [66]. Even though the dispersion of the data (with respect to the presented fitting line) seems slighter than the one evidenced when assessing TPPCA (in Figure 4.34), the R^2 values suggest the opposite.

$$TPPCW = -0.346 \times LPP + 849 \quad [66]$$

Once again, a clear change on the overall TPPCW behaviour is observed at around LPP values of 200 m. The set of shorter vessels depicts a clear decrease in TPPCW with increasingly higher LPP values, while the set of longer vessels shows a constant TPPCW throughout the considered LPP range. This is due to the different ship types associated with each LPP set, as mentioned in Chapter 4.3.1.

It's interesting to see how, in the conditions defined in Chapter 3.6, the profitability of production is affected differently, depending on the defining variable. The results presented in terms of TPPCA show that the profitability with respect to panel area decreases for larger vessels. Oppositely, the TPPCW results depict an increase in profitability with respect to panel weight for larger vessels. This means that while producing a squared meter of stiffened panel gets more expensive for vessels with increasingly higher LPP values, producing a ton of stiffened panel gets cheaper for larger vessels.

The TPPCW results for bulk carrier vessels as a function of LPP are displayed in Figure 4.43.

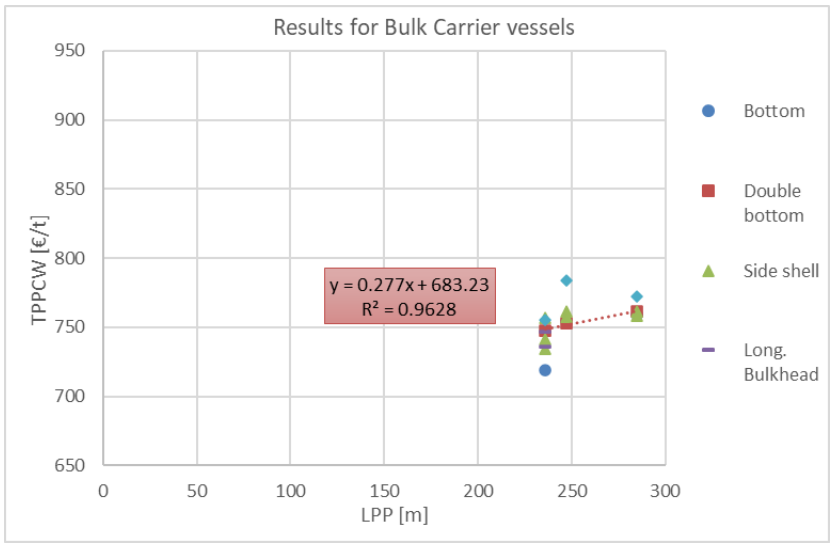

Figure 4.43. TPPCW [€/t] as a function of LPP [m] for bulk carrier vessels

Surprisingly, and considering the overall results shown in Figure 4.42 (which presented a decrease in TPPCW with the increase in LPP), the results for bulk carrier vessels present a general trend of increase in TPPCW with increasing LPP values. Namely, this trend can be assessed in the fitting line expression for double bottom panels presented in Equation [67].

$$TPPCW = 0.277 \times LPP + 683 \quad [67]$$

It must be pointed out that the observed increase is very slight, as the axis relative to the costs had to be defined to go from 650 €/t to 810 €/t for better visualization. If the same plot resolution as in Figure 4.42 had been adopted, it wouldn't be possible to evaluate any sort of variation.

The results of TPPCW as a function of LPP for container carrier vessels are depicted in Figure 4.44.

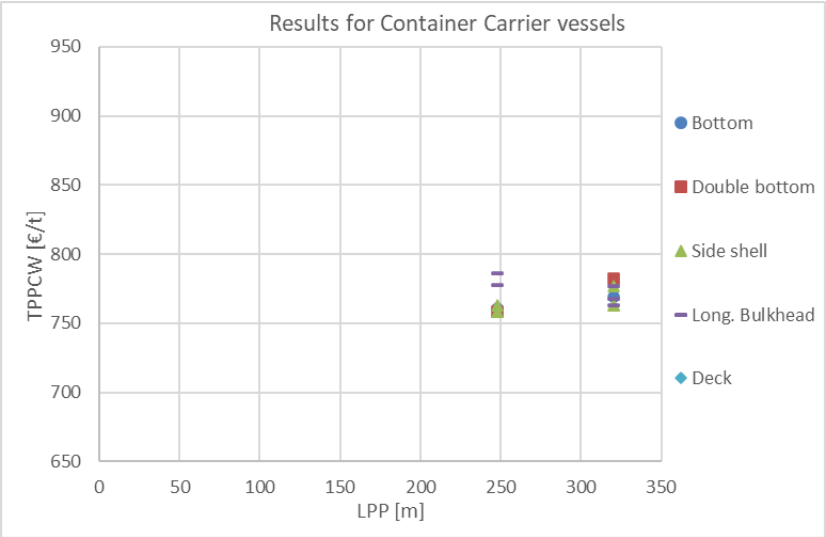

Figure 4.44. TPPCW [€/t] as a function of LPP [m] for container carrier vessels

The TPPCW results for container carrier vessels presented in Figure 4.44 show an overall constant behaviour. As mentioned, when analogizing the TPPCA for container carrier vessels (Figure 4.36), the scarcity of data entries regarding container carrier panels can lead to unjustified conclusions regarding the global behaviour of this ship type.

The multipurpose vessel results regarding the influence of LPP on the TPPCW are shown in Figure 4.45.

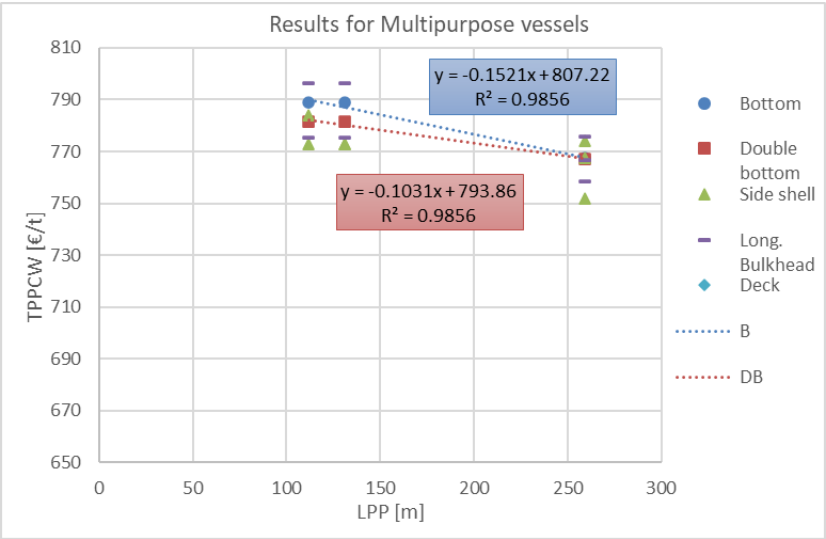

Figure 4.45. TPPCW [€/t] as a function of LPP [m] for multipurpose vessels

A clear linear decrease in the TPPCW with increasing LPP values is observed. Besides, this behaviour is even observed at a panel-level, as several multipurpose vessel panel types present the mentioned decrease in costs with increasing LPP values. This becomes clear when evaluating the results and the fitting lines for bottom and double bottom panels (Equations [68] and [69], correspondingly).

$$TPPCW = -0.152 \times LPP + 807 \quad [68]$$

$$TPPCW = -0.103 \times LPP + 794 \quad [69]$$

The TPPCW results as function of LPP for passenger vessels are shown in Figure 4.46.

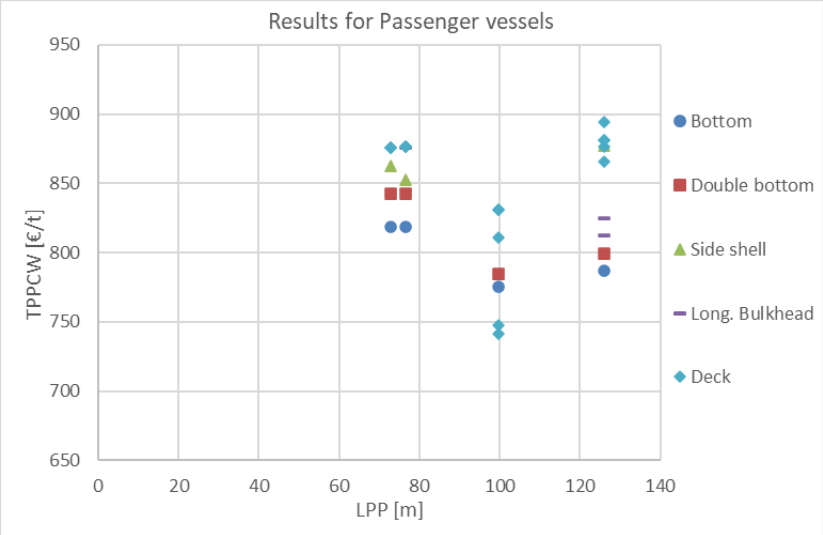

Figure 4.46. TPPCW [€/t] as a function of LPP [m] for passenger vessels

No overall pattern regarding the variation of TPPCW as a function of LPP is observed, when considering every passenger vessel panel.

When considering the behaviour of each panel type individually, one can observe an interesting trend, which is specifically evident in the case of bottom and double bottom panels. For these panel types, and considering increasing LPP values, the results show a decrease in TPPCW, reaching a local minimum and followed by an increase in TPPCW. This sort of parabolic tendency is visibly enhanced by the plot resolution adopted in Figure 4.46. Considering the results for all panels presented in Figure 4.42, such tendency becomes almost insignificant regarding the overall pattern of decreasing TPPCW with increasing LPP values.

Figure 4.47 presents the TPPCW results as function of LPP for tanker vessels.

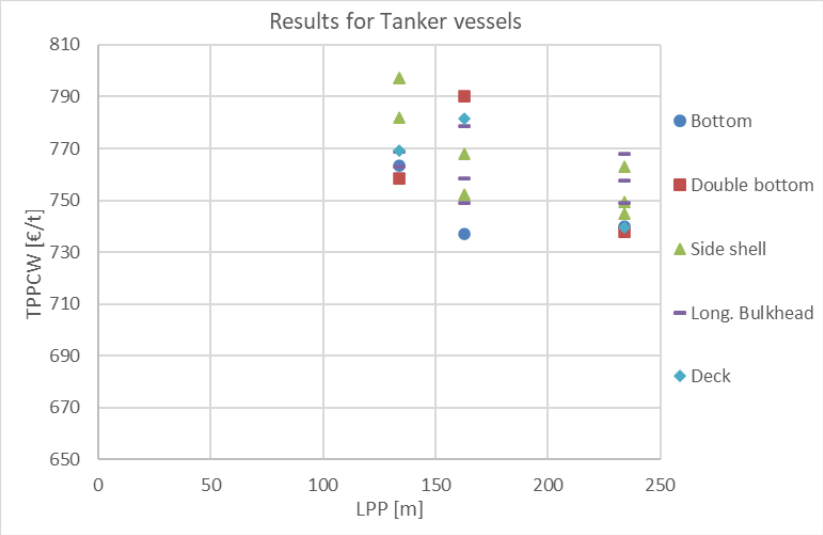

Figure 4.47. TPPCW [€/t] as a function of LPP [m] for tanker vessels

The observed tendency is of overall decrease of TPPCW with increasingly higher LPP values. This behaviour is in line with the overall tendency that is observed when no distinction is made regarding ship type. However, some dispersion is found, namely for lower LPP values, with deck panels even presenting a local maximum around 780 €/t.

To sum up, the general behaviour observed in Figure 4.42, which depicts a slight decrease in TPPCW with increase in LPP, is also observed for multipurpose and tanker vessels. However, different situations are also visible, when regarding other ship types. Bulk carrier vessels, for instance, show an increase in TPPCW with increasing LPP values, while TPPCW for container carrier vessels tend to remain constant despite increasing LPP values.

4.3.4. Panel production costs per unit weight: a comparative analysis regarding bottom panels production costs

In the present chapter, the ratio between the TPPCW of each panel type and the TPPCW of the corresponding bottom panel is analysed as a function of LPP. The mentioned ratio is presented below, in Equation [70].

$$\frac{TPPCW_{chosen\ panel}^{ship\ n}}{TPPCW_{bottom\ panel}^{ship\ n}} \quad [70]$$

This evaluation will allow to establish an understanding on how the TPPCW of each panel type compares to the TPPCW of bottom panels.

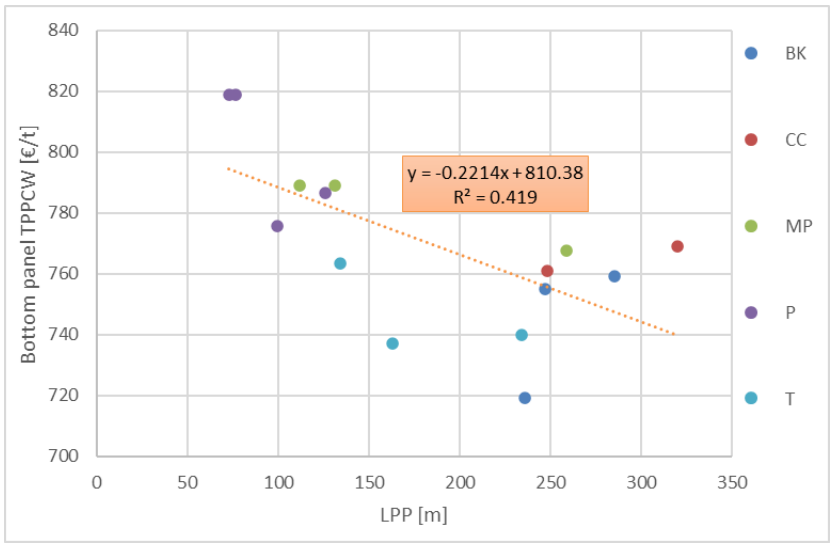

Figure 4.48. TPPCW [€/t] as a function of LPP [m] for bottom panels

This comparison is of significant interest, considering the usual higher strength of bottom panels with respect to other ship panel types. The TPPCW results for bottom panels presented in Figure 4.48 show a decrease on bottom TPPCW with the increase in LPP (this can be assessed using the shown overall fitting line expression, Equation [71]).

$$TPPCW = -0.221 \times LPP + 810 \qquad [71]$$

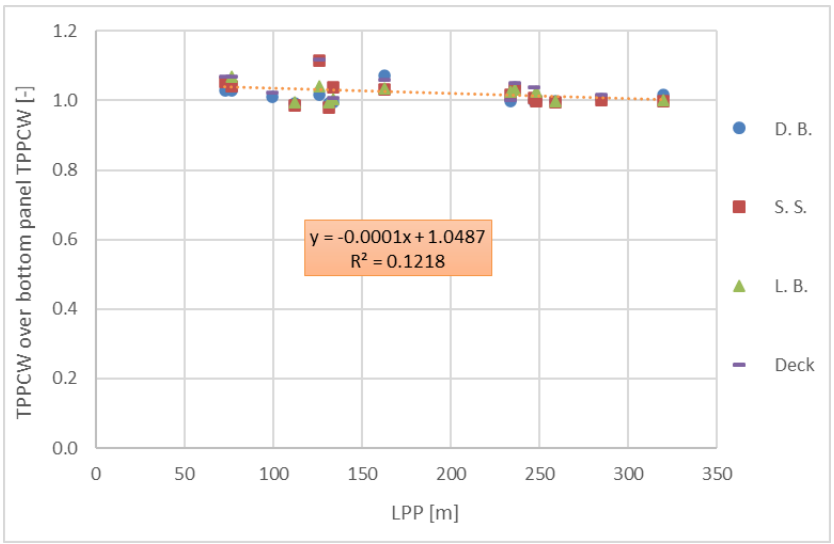

Figure 4.49. TPPCW over bottom TPPCW as a function of LPP [m]

The results shown in Figure 4.49 translate one clear global tendency. For all the panel types considered in this study, the ratio between each TPPCW and bottom TPPCW remains asymptotically constant around the value of 1. The fitting line expression for all the considered panels, disregarding panel types, is presented in Equation [72] and shows exactly that. It is interesting to observe how such distinct types

of panels present the same cost as the corresponding bottom panels, throughout the entire scope of considered LPP values.

$$\frac{TPPCW}{TPPCW_{bottom}} = -0.0001 \times LPP + 1.05 \quad [72]$$

5. Conclusions and Future work

5.1. Conclusions

The implementation of the ships and ship panels databases led to important conclusions at both global and local level, in areas as distinct as ship structural behaviour and shipbuilding production costs.

The results obtained when assessing how stiffened panel strength was influenced by LPP showed a clear proportional increase in panel strength with increasingly higher LPP values. This tendency was evident in all the considered panel types, with interesting distinctive aspects being found in some of them. Both bottom and double bottom panel types presented a linear increase in panel strength up to LPP values around 200 m. For larger vessels, the panel strength would then reach an asymptotic value, and even decrease eventually (this was observed for double bottom panels). The similarities between the results regarding these panel types are due to equal stiffener spacings and similar distances relatively to the midship section neutral axis. These distances define the bending stress loads that affect the structural design process more significantly, leading to similar panel strength tendencies. An interesting fact was also observed in the assessment of the panel strength results for deck panels: much higher values of panel strength were observed for cargo vessels (namely bulk carriers and tankers) when in comparison to passenger vessels. An explanation for this can come from the significant difference in magnitude of the loads considered for the design of, for example, a tanker (with the amount of heavy machinery and structural reinforcements required for several compliances) when compared to a passenger vessel, (expected to withstand not much more than the passengers).

When evaluating the influence of the panel aspect ratio, α, on the stiffened panel strength, bottom, double bottom, side shell and longitudinal bulkhead panels presented a cluster-like behaviour. This means that most panel strength results were dispersed around a given central value, with α values ranging from 3 to 5. The concentration of α values showed that in the design of different types of ships and ship panels, some geometrical relations (in this case the ratio between panel length and width) tend to be quite similar. This similarity can be due to the fact that this range of α values is somewhat optimal for the structure's integrity.

The study on the influence of the corrosion additions on panel strength, led to clear conclusions. When deducting the corrosion additions to both plate and stiffener thicknesses, a general decrease in stiffened panel strength was observed, when comparing to the values obtained considering the original thicknesses.

The local strength assessment led to two main conclusions: there's a general pattern of decrease in maximum bending stress over lateral pressure ratio with the increase in LPP and a visible increase in the pressure to reach bending yield stress with the increase in LPP. These results showed how, in comparison to smaller vessels, larger vessels develop lower bending stresses when subjected to a given lateral pressure and are able to withstand higher local lateral pressures to reach the respective bending

yield stress. Regarding the ratio between maximum bending stress and lateral pressure, certain panel types presented relevant differences depending on the considered LPP range. For instance, double bottom panels presented a more significant decrease of the maximum bending stress in smaller vessels, stabilizing around a plateau for larger vessels. This behaviour is related to the difference between the structural approach at a global (stiffened panel strength) and local (local strength assessment) level. For smaller vessels, the local approach was more significant, while for larger vessels, the global approach considering longitudinal bending defined the design process. The increase in LPP won't translate into further decrease in the maximum bending stress (hence the observed plateau), as vessels with these LPP values were only affected at a global panel strength level.

Concerning the influence of panel aspect ratio (α) on the local strength assessment, the results showed an overall tendency of increase in maximum bending stress over lateral pressure, with an increase in α and an overall tendency of decrease in the pressure to reach bending yield stress with increasingly higher α values. From these observations, it was possible to conclude that stockier panels (presenting lower α values) are better prepared to withstand higher lateral pressures, being able to withstand higher pressures than slenderer panels for the same stress level. It was also interesting to assess how the position of the considered panel affected the local strength assessment. For longitudinal bulkhead panels, the pressures to reach bending yield stress are significantly lower than, for instance, for bottom panels, due to the distance between the panel and the corresponding midship section neutral axis (which is higher for bottom panels, in most cases). As previously mentioned, this aspect affects the loads the panel must endure, subsequently affecting the structural design.

The study on the influence of corrosion additions on the local strength assessment, showed an increase in maximum bending stress over lateral pressure ratio and a corresponding drop on the pressures to reach bending yield stress, when deducting the corrosion additions from the original thicknesses. Due to the significant decrease in the amount of structural material, it was expected for the structure to present higher stresses for the same load case and reaching bending yield stress with lower lateral pressures applied. Both situations were verified in the assessment results.

Further studies allowed to verify a clear tendency of linear increase in TPPCA with increasingly higher LPP values, for LPP values up to around 200 m. Nevertheless, for LPP values higher than 200 m, the TPPCA appeared to remain constant despite the increase in LPP. These distinct trends have to do with the two different LPP ranges that define the ship types considered in the ship database (the lowest LPP range is associated with passenger and multipurpose vessels and the highest LPP range is associated with tanker, bulk and container carrier vessels). Even though no particular trend can be assessed as common to every ship type or panel type, ship types such as multipurpose and tanker vessels presented a linear increase in TPPCA with an increase in LPP across all the considered panel types. Contrarily, some of the panel types associated with bulk carriers, namely bottom, double bottom, and side shell panels, presented a decrease in TPPCA with an increase in LPP. Besides, it was observed how for double bottom, side shell and longitudinal bulkhead panels the ratio between each TPPCA and

respective bottom TPPCA remained asymptotically constant throughout the entire LPP scope (around 1). This shows how, regardless of the considered ship type, the TPPCA of a given panel will generally equal the TPPCA of the corresponding bottom panel.

Overall, the studies regarding TPPCW showed a slight decrease in TPPCW with the increase in LPP. This result was of particular interest, as results presented in terms of TPPCA showed that the profitability with respect to panel area decreases for larger vessels, while the TPPCW results depict an increase in profitability with respect to panel weight for larger vessels. This behaviour was also observed at a ship type level, with multipurpose and tanker vessels presenting a decrease in TPPCW with the increase in LPP. However, different situations were also visible when regarding other ship types. Bulk carrier vessels showed an increase in TPPCW with increasing LPP values, while TPPCW for container carrier vessels tend to remain constant despite increasing LPP values. When assessing the ratio between TPPCW for a given panel and TPPCW for the respective bottom panel, it was observed how this ratio remained around 1 throughout the entire LPP scope. Once again this depicted how, independently of the considered ship type, the TPPCW for a given panel will be the same as for the bottom panel.

5.2. Future work

Even though the studies carried out in the present dissertation allowed to reach important conclusions and showed how data analysis can be implemented in the ship design process, some improvements can be made in future works.

To improve the results obtained in the present thesis, one would have to significantly increase the number of ships, and consequently panel data, present on the ships and ship panels databases, respectively. This would allow for a more clear and concise understanding of some of the observed patterns, as with the increase in the amount of data analysed, the uncertainty present on the conclusions drawn would decrease.

Besides, it would be interesting to include ship types different than the ones considered thus far. The inclusion of a larger variety of ship types (namely naval, offshore, among other types of vessels) would enable a verification on whether such distinct ship types could be compared when assessing their properties.

Finally, and considering that one of the main objectives of a database is its reusability, the implementation of different studies using the gathered data could furthermore prove how useful this database is, regardless of the type of analysis carried out.

6. References

[1] L. Columbus, ‘Global State Of Enterprise Analytics, 2018’, *Forbes*, Aug. 08, 2018.

[2] ‘2018 Global State of Enterprise Analytics Report’, MicroStrategy.

[3] S.-H. Kim, M.-I. Roh, M.-J. Oh, S.-W. Park, and I.-I. Kim, ‘Estimation of ship operational efficiency from AIS data using big data technology’, *Int. J. Nav. Archit. Ocean Eng.*, vol. 12, pp. 440–454, 2020.

[4] K. A. Hossain and N. M. G. Zakaria, ‘A Study on Global Shipbuilding Growth, Trend and Future Forecast’, *Procedia Eng.*, vol. 194, pp. 247–253, 2017, doi: 10.1016/j.proeng.2017.08.142.

[5] O. Ozguc, ‘Modelling aspects for reduced stiffness in bulk carrier vessels’, *Ocean Eng.*, vol. 216, Nov. 2020, doi: 10.1016/j.oceaneng.2020.107845.

[6] G. Wang, A.-K. Lee, L. Ivanov, T. J. Lynch, C. Serratella, and R. Basu, ‘A statistical investigation of time-variant hull girder strength of aging ships and coating life’, *Mar. Struct.*, vol. 21, no. 2–3, pp. 240–256, Jul. 2008, doi: 10.1016/j.marstruc.2007.10.002.

[7] T. A. Kletz, ‘Zeebrugge’, in *Critical Aspects of Safety and Loss Prevention*, Butterworth-Heinemann, 1990.

[8] ‘Revised Guidelines for Formal Safety Assessment (FSA) for use in the IMO rule-making process’. International Maritime Organization, Apr. 09, 2018. [Online]. Available: shorturl.at/elJN6

[9] Y. Bai and W.-L. Jin, ‘Chapter 49 - Explosion and Fire Response Analysis for FPSO’, in *Marine Structural Design*, 2nd ed., 2015, pp. 907–938.

[10] D. Shallcross, ‘Using concept maps to assess learning of safety case studies – The Piper Alpha disaster’, *Educ. Chem. Eng.*, vol. 8, no. 1, pp. 1–11, May 2013, doi: 10.1016/j.ece.2013.02.001.

[11] ‘CSA S471’. CSA Group, Dec. 2008.

[12] P. R. Brand, W. S. Whitney, and D. B. Lewis, ‘Load and Resistance Factor Design Case Histories’, presented at the Offshore Technology Conference, Houston, Texas, May 1995. doi: 10.4043/7937-MS.

[13] T. V. Galambos and M. K. Ravindra, ‘Load and Resistance Factor Design Criteria for Composite Beams’, Washington University, St. Louis, MO, Research Report 44, 1976.

[14] ‘UR I - Requirements concerning Polar Class’. IACS, 2019. [Online]. Available: https://www.iacs.org.uk/publications/unified-requirements/ur-i/

[15] J. B. Caldwell, ‘Ultimate longitudinal strength’, *Trans RINA*, vol. 107, pp. 411–430, 1965.

[16] D. Faulkner, ‘A review of effective plating for use in the analysis of stiffened plating in bending and compression’, *J. Ship Res.*, vol. 19, no. 1, pp. 1–17, Mar. 1975, doi: 10.5957/jsr.1975.19.1.1.

[17] D. W. Billingsley, ‘Hull girder response to extreme bending moments’, 1980, pp. 51–63.

[18] J. C. Adamchak, ‘An approximate method for estimating the collapse of a ship’s hull in preliminary design’, 1984, pp. 37–61.

[19] Y. T. Lin, ‘Ship longitudinal strength’, Ph.D. thesis, University of Glasgow, Scotland, 1985.

[20] S. E. Rutherford and J. B. Caldwell, ‘Ultimate longitudinal strength of ships: a case study’, *Trans SNAME*, vol. 98, pp. 441–471, 1990.

[21] J. M. Gordo and C. Guedes Soares, ‘Approximate load shortening curves for stiffened plates under uniaxial compression’, in *Integrity of Offshore Structures - 5*, Warley, U.K.: EMAS, 1993, pp. 189–211.

[22] D. Faulkner, J. C. Adamchak, M. Snider, and M. F. Vetter, ‘Synthesis of welded grillages to withstand compression and normal loads’, *Comput. Struct.*, vol. 3, pp. 221–246, 1973, doi: 10.1016/0045-7949(73)90015-1.

[23] J. M. Gordo, I. Carvalho, and C. G. Soares, ‘Potencialidades de processos tecnológicos avançados de corte e união de aço em reparação naval’, in *Inovação e Desenvolvimento nas Actividades Marítimas*, Edições Salamandra, 2006, pp. 877–890.

[24] T. Ohno, *Toyota production system: beyond large-scale production*. 1988.

[25] R. Storch and S. Lim, ‘Improving flow to achieve lean manufacturing in shipbuilding’, *Prod. Plan. Control*, vol. 10, no. 2, pp. 125–137, 1999, doi: 10.1080/095372899233280.

[26] J. Liker and T. Lamb, ‘What is lean ship construction and repair?’, *J. Ship Prod.*, vol. 18, no. 3, pp. 121–142, Aug. 2002, doi: 10.5957/jsp.2002.18.3.121.

[27] M. Leal and J. M. Gordo, ‘Hull’s manufacturing cost structure’, *Brodogradnja*, vol. 68, no. 3, pp. 1–24, Sep. 2017, doi: 10.21278/brod68301.

[28] B. Ljubenkov, G. Dukié, and M. Kuzmanié, ‘Simulation Methods in Shipbuilding Process Design’, *J. Mech. Eng.*, vol. 54, pp. 131–139, 2008.

[29] A. Oliveira and J. M. Gordo, ‘Lean tools applied to a shipbuilding panel line assembling process’, *Brodogradnja*, vol. 69, no. 4, pp. 53–64, Dec. 2018, doi: 10.21278/brod6944.

[30] C.-K. Lin and H.-J. Shaw, ‘Feature-based estimation of preliminary costs in shipbuilding’, *Ocean Eng.*, vol. 144, pp. 305–319, 2017, doi: 10.1016/j.oceaneng.2016.11.040.

[31] C. Guedes Soares, Y. Garbatov, and K. T. Nguyen, ‘Fatigue Damage Assessment of a Tanker Structural Detail Based on the Effective Notch Stress Approach’, in *Maritime Engineering and Technology*, London: Taylor & Francis Group, 2012, pp. 363–373.

[32] ‘Common Structural Rules for Bulk Carriers and Oil Tankers’. IACS, Jan. 01, 2021.

[33] ‘Rules for Ships’. DET NORSKE VERITAS, Jan. 1997.